Nature Communications

https://doi.org/10.1038/s41467-026-71474-0

Article in Press

ZFP36L2 is an interferon β -induced inhibitor that restricts the nuclear export of HIV-1 transcripts

Received: 27 August 2025

Accepted: 17 March 2026

Cite this article as: Pang, H., Cui, H., Yin, X. *et al.* ZFP36L2 is an interferon β -induced inhibitor that restricts the nuclear export of HIV-1 transcripts. *Nat Commun* (2026). https://doi.org/10.1038/s41467-026-71474-0

Hailin Pang, Hualu Cui, Xiaowan Yin, Zengwen Yang, Hong Shang & Guoxin Liang

ZFP36L2 is an interferon β -induced inhibitor that restricts the nuclear export of HIV-1 transcripts

Hailin Pang[1,2,†], Hualu Cui[1,3,†], Xiaowan Yin[1,2], Zengwen Yang[1,3], Hong Shang[1,2,3,4,*], and Guoxin Liang[1,2,3,5*]

[1]State Key Laboratory for Diagnosis and Treatment of Infectious Diseases, National Health Commission Key Laboratory of AIDS Prevention and Treatment, The First Hospital of China Medical University, Shenyang110001, China

[2]National Clinical Research Center for Medical Auxiliary (Laboratory Medicine), Department of Laboratory Medicine, The First Hospital of China Medical University, Shenyang110001, China

[3]Key Laboratory of AIDS Immunology, Chinese Academy of Medical Sciences, Shenyang 110001, China

[4]Collaborative Innovation Center for Diagnosis and Treatment of Infectious Diseases, 79 Qingchun Street, Hangzhou 310003, China

[5]Center for Cell and Gene Therapy, The First Hospital of China Medical University, Shenyang110001, China

[†]These authors contributed equally

*Corresponding author:

Hong Shang: hshang@cmu.edu.cn

Guoxin Liang: gxliang@cmu.edu.cn

Phone: +86-2483282634; Fax: +86-2483282634

Abstract

Type I interferons restrict HIV-1 replication by inducing antiviral genes, but the full spectrum of their effectors remains incompletely defined. Here we identify ZFP36L2, a nuclear RNA-binding protein, as an IFN-β-induced inhibitor of HIV-1 infection. Silencing of *ZFP36L2* impairs IFN-β-mediated HIV-1 inhibition, whereas overexpression of ZFP36L2 suppresses viral replication. Notably, reconstitution of ZFP36L2 in $CD4^+$ T cells from HIV-1-infected individuals reduces viral spread *ex vivo*, and ZFP36L2 transcript levels inversely correlate with plasma viral loads *in vivo*. Mechanistically, ZFP36L2 binds to the HIV-1 Rev protein and inhibits the nuclear export of Rev response element-containing viral transcripts, thereby blocking downstream viral protein expression. A Rev mutant lacking amino acids 109–116 fails to bind ZFP36L2 and exhibits resistance to ZFP36L2-mediated inhibition, underscoring the functional significance of this interaction. These findings establish ZFP36L2 as an IFN-β-induced antiviral factor that suppresses HIV-1 replication through Rev-dependent inhibition of viral RNA export.

Introduction

Human immunodeficiency virus (HIV-1) infection in humans induces innate immune responses that are primarily mediated by type I interferons (IFN-Is), which are antiviral cytokines comprising 12 different IFN-α subtypes and IFN-β. They exert broad antiviral effects by activating interferon-stimulated genes (ISGs) [1-9]. Upon HIV-1 infection, pattern recognition receptors and cytosolic sensors in human immune cells detect viral cDNA and RNA. Viral cDNA is first recognized by IFN-inducible protein 16 (IFI16) or cyclic GMP–AMP (cGAMP) synthase, triggering IFN-I production via IFI16 and the cGAMP-activating stimulator of the IFN gene (STING) [10-13]. Extensive *in vitro* studies have identified several ISGs, such as IFN-induced transmembrane proteins (IFITMs), APOBEC3G, Tetherin, SAMHD1, MX2, and Shiftless that exert potent anti-HIV-1 activity [8, 9, 14-23]. These findings suggest that IFN-I responses triggered by HIV-1 infection play a crucial role in limiting viral spread.

HIV-1 gene expression is regulated by several posttranscriptional mechanisms, including RNA splicing, stability, transport, and translation. Because the HIV-1 genome contains an AU-rich sequence, rapid nuclear export facilitated by the Rev protein is necessary to prevent excessive splicing. The HIV-1 Rev response element (RRE), a ~350 bp, highly structured RNA element located within the *env*-coding region of the viral genome, is essential for viral replication and is highly conserved across different HIV-1 isolates. During the late phase of the viral life cycle, viral proteins are translated from unspliced (9 kb) and partially spliced (4 kb) RRE-containing RNAs. These intron-containing RNAs are typically retained in the nucleus for splicing or degradation. However, their nuclear export is achieved through the cooperative binding of multiple Rev molecules to the RRE. This assembly recruits the host Crm1/Ran-GTP nuclear export machinery via

the nuclear export signal of Rev. Once in the cytoplasm, these RNAs are either translated into viral proteins or packaged as genomic RNA for new virions. Notably, HIV-1 infection occurs in activated $CD4^+$ T cells, where cytokine and chemokine mRNA decay is regulated by the binding of AU-rich elements to the mRNA-destabilizing protein ZFP36 (tristetraprolin). ZFP36 belongs to a family of CCCH zinc finger-containing RNA-binding proteins, which includes ZFP36L1 and ZFP36L2 [24, 25]. These human ZFP36 family proteins contain two conserved zinc finger domains and typically bind to adenine-uridine (AU)-rich elements (AREs) in the 3′ untranslated region (3′-UTR) of cytokine mRNAs, exerting anti-inflammatory activity via transcript destabilization [25-30]. Moreover, ZFP36 antagonizes Myc-induced lymphomagenesis [31], while its paralogs, ZFP36L1 and ZFP36L2, play redundant roles in preventing T cell leukemia in mice and promoting cell quiescence [32, 33]. Furthermore, ZFP36 directly inhibits HIV-1 production by binding to genomic RNA [34], while ZFP36L1 inhibits influenza A virus replication through translational repression by selectively targeting viral RNA [35].

In this study, we identified ZFP36L2 as a downstream effector of IFN-β but not IFN-α that mediates the inhibition of HIV-1 infection. Our findings reveal that IFN-β significantly induces ZFP36L2 expression in $CD4^+$ T lymphocytes and macrophages. Notably, ZFP36L2 overexpression reduces susceptibility to multiple lentiviruses, including HIV-1, HIV-2, simian immunodeficiency virus (SIV), and equine infectious anemia virus (EIAV), but not to feline immunodeficiency virus (FIV) or murine leukemia virus (MLV). In addition, ZFP36L2 overexpression restricts *ex vivo* HIV-1 spread in $CD4^+$ T cells from HIV-1-infected individuals. In untreated HIV-1-infected individuals, ZFP36L2 transcript levels in $CD4^+$ T cells inversely correlated with viral loads. Conversely, ZFP36L2 depletion via

RNA interference (RNAi) diminished the anti-HIV-1 activity of IFN-β in $CD4^+$ T cells and macrophages. Mechanistic studies revealed that ZFP36L2 inhibits the nuclear export of RRE-containing viral transcripts by interacting with the HIV-1 Rev protein. Therefore, ZFP36L2 is a critical effector of the anti–HIV-1 activity mediated by type I IFN-β, shedding light on the intricate molecular mechanisms underlying the IFN-β–driven antiviral response against HIV-1.

Results

ZFP36L2 restricts HIV-1 infection

To investigate the potential anti-HIV activity of the ZFP36 family—given that ZFP36 inhibits HIV-1 production by binding to viral genomic RNA—we first overexpressed its family members, ZFP36, ZFP36L1 and ZFP36L2, along with the proviral vector $HIV\text{-}1_{NL4\text{-}3}$ in 293T cells and assessed viral production. All members of the ZFP36 family could inhibit HIV-1 titers (Supplementary Fig. 1a) when expressed at comparable protein levels, with ZFP36L2 exhibiting the most potent inhibitory effect. Subsequently, we further investigated the anti-HIV activity of ZFP36L2 by coexpressing it with the $HIV\text{-}1_{NL4\text{-}3}$ proviral vector in 293T cells. Viral titers were significantly reduced in a dose-dependent manner, with a 15- to 41.5-fold decrease with increasing ZFP36L2 expression levels (Fig. 1a,b). Notably, Gag and Env levels were reduced, whereas Nef levels remained unaffected regardless of ZFP36L2 expression. These findings suggest that ZFP36L2 inhibits the production of HIV-1 progeny virions in producer cells without altering Nef protein levels. Next, we assessed ZFP36L2 against other HIV-1 isolates, including the CCR5-tropic BaL and AD8, and dual-tropic 89.6. In all cases, p24 levels were decreased

in the presence of ZFP36L2 (Fig. 1c), indicating that ZFP36L2 inhibits the production of progeny virions across these HIV-1 strains. Moreover, exogenous ZFP36L2 consistently inhibited HIV-1 progeny virion production in stimulated $CD4^+$ T lymphocytes (Fig. 1d).

To determine whether ZFP36L2 could restrict HIV-1 spread in T cells, we generated ZFP36L2-expressing Jurkat T cells using lentiviral vectors. HIV-1 spread was significantly inhibited in ZFP36L2-expressing Jurkat T cells compared to GFP-expressing control cells (Supplementary Fig. 1c–e). Notably, ZFP36L2 expression did not evidently affect cell proliferation (Supplementary Fig. 1c), indicating that the observed inhibitory effect was due to ZFP36L2 and not cell toxicity. Similarly, in stimulated primary $CD4^+$ T lymphocytes, ZFP36L2 effectively restricted viral spread (Fig. 1e–g). To further substantiate these findings, we examined the effect of ZFP36L2 on HIV-1 spread in primary macrophages. Consequently, ZFP36L2 inhibited the spread of CCR5-tropic HIV-1 in nondividing primary macrophages (Fig. 1h,i). Furthermore, we also examined lactate dehydrogenase (LDH) release as a measure of toxicity and found no significant toxicity associated with ZFP36L2 expression (Fig. 1j), thereby confirming that the observed inhibition of HIV-1 proliferation in the presence of ZFP36L2 is not due to cell toxicity.

Next, we determined whether ZFP36L2 exhibits broad antiviral activity. We challenged ZFP36L2-overexpressing cells with HIV-2, SIV, FIV, MLV, and HBV. Our findings demonstrated that ZFP36L2 inhibited HIV-1, HIV-2, and SIV, but had no significant effect on FIV, MLV, or HBV. Specifically, ZFP36L2 strongly inhibited the titers of $HIV\text{-}2_{Rod}$ (Fig. 1k), SIV_{mac239} (Fig. 1l), and EIAV (Fig. 1m) in producer cells. However, no significant inhibitory effect was observed for FIV, MLV, or HBV titers (Fig. 1n–p). These findings suggest that ZFP36L2 preferentially restricts primate lentiviruses and does not

exhibit broad-spectrum antiviral activity against retroviruses. The mechanism underlying the resistance of FIV and MLV to ZFP36L2-mediated inhibition requires further investigation.

IFN-β induces ZFP36L2 expression

We assessed endogenous ZFP36L2 expression across multiple cell types and found it to be constitutively expressed in primary macrophages, monocytes, and PMA-stimulated THP-1 cells. Lower levels of ZFP36L2 were detectable in stimulated $CD4^+$ T lymphocytes and dendritic cells, whereas ZFP36L2 expression was undetectable in 293T, HeLa, and Jurkat cell lines (Supplementary Fig. 2a). To investigate interferon regulation, stimulated $CD4^+$ T cells were treated with IFN-α, IFN-β, or IFN-γ. Among these, only IFN-β robustly induced ZFP36L2 expression (Supplementary Fig. 2b,c). A similar trend was observed in primary macrophages, where IFN-β further enhanced the already high basal ZFP36L2 levels. IFN-γ induced a modest upregulation, while IFN-α had no significant effect on ZFP36L2 expression (Supplementary Fig. 2d,e). We next examined whether other members of the ZFP36 family are responsive to interferon signaling. In both stimulated $CD4^+$ T cells and macrophages, only ZFP36L2—not ZFP36 or ZFP36L1—was significantly upregulated by IFN-β (Supplementary Fig. 2f,g), suggesting ZFP36L2 as the primary IFN-β-responsive member in these cells. Consistently, among the ZFP36 family proteins, ZFP36L2 exhibited the strongest anti-HIV-1 activity when overexpressed (Supplementary Fig. 1a,b), suggesting its distinct role in IFN-β-mediated antiviral defense.

To compare ZFP36L2 regulation with that of MX2, a well-established IFN-I-induced HIV-1 restriction factor, we analyzed the expression kinetics of both genes in response to

interferon stimulation. While IFN-α and IFN-β strongly induced MX2 in $CD4^+$ T cells and macrophages, only IFN-β significantly upregulated ZFP36L2 (Supplementary Fig. 2h,i). ZFP36L2 and MX2 showed distinct induction profiles: MX2 peaked at 12 h and declined thereafter, whereas ZFP36L2 expression gradually increased, peaking at 48 h poststimulation. These kinetic differences were leveraged in subsequent IFN-β experiments to specifically study ZFP36L2-mediated antiviral activity.

ZFP36L2 Inhibits the nuclear export of RRE-containing HIV-1 transcripts

To investigate the molecular mechanism by which ZFP36L2 inhibits HIV-1 production, we first examined whether it affects the early stages of the viral replication cycle. Using $HIV\text{-}1_{NL4\text{-}3.Luc.\ R^-.E^-}$ reporter vectors, we found that ZFP36L2 did not reduce luciferase activity in producer cells (Fig. 2a). Next, we separated nuclear and cytoplasmic fractions from 293T cells. Although total Gag RNA levels remained unchanged, cytoplasmic Gag RNA levels were markedly reduced (by approximately 11.9-fold), while nuclear Gag RNA levels increased (by approximately 2.1-fold) in the presence of ZFP36L2 (Fig. 2b). These changes are consistent with a model in which ZFP36L2 impairs the nuclear export of HIV-1 Gag RNA. This result supports the conclusion that ZFP36L2 blocks the nuclear export of Gag RNA, leading to its nuclear accumulation. The separation of nuclear and cytoplasmic fractions was validated using the following protein markers— Lamin B (nuclear), GAPDH (cytoplasmic), and p24Gag (viral) (Fig. 2c, left) —as well as the nuclear RNA marker U6 RNA (Fig. 2c, right). Moreover, reverse transcription-negative RT-qPCR did not yield any amplification, confirming the absence of contamination from proviral DNA (Fig. 2b). These findings suggest that ZFP36L2 restricts the cytoplasmic transport of Gag

RNA, promoting its nuclear retention. Consistent effects were observed in Jurkat T cells (Supplementary Fig. 3a–c) and $CD4^+$ T lymphocytes (Supplementary Fig. 3d–f), where ZFP36L2 similarly reduced cytoplasmic and increased nuclear Gag RNA levels. To determine whether ZFP36L2 directly targets Gag RNA, we cloned the Gag sequence into an exogenous expression vector and cotransfected it with ZFP36L2 into 293T cells. In this context, ZFP36L2 did not affect the nuclear export of exogenous Gag RNA (Supplementary Fig. 3g), indicating that its activity requires specific HIV-1 cis-acting elements.

We then analyzed different HIV-1 transcript classes derived from the wild-type $HIV\text{-}1_{NL4\text{-}3}$ proviral vector (Fig. 2d) in the presence or absence of ZFP36L2. In the cytoplasm, ZFP36L2 selectively reduced unspliced (gag-pol) and singly spliced (vif, vpr, vpu/env) transcript levels, whereas those of multiply spliced transcripts (tat, rev, nef) remained unaffected (Fig. 2e). Conversely, in the nucleus, gag-pol and singly spliced transcript levels increased, whereas those of multiply spliced transcripts remained unchanged. The total RNA levels of all transcript classes (gag-pol, vif, vpr, vpu/env, tat, rev, and nef) were unaffected, indicating that ZFP36L2 selectively inhibits the nuclear export of unspliced and singly spliced transcripts without altering their synthesis or stability. To validate these findings, we performed RT-PCR followed by Southern blotting using primers (forward primer FP; reverse primers RP1 and RP2, as indicated) that amplify all singly and multiply spliced HIV-1 transcripts (Fig. 2f). Consistently, ZFP36L2 expression significantly reduced cytoplasmic levels and increased nuclear levels of singly spliced transcripts, whereas multiply spliced transcripts remained unaffected in both

compartments (Fig. 2g). Proper cellular fractionation was confirmed by analyzing compartment-specific protein markers and U6 snRNA (Fig. 2h,i). Notably, the HIV-1 RRE is present in unspliced and singly spliced transcripts but absent from multiply spliced transcripts (Fig. 2d), suggesting that ZFP36L2 specifically targets and inhibits the nuclear export of RRE-containing transcripts, thereby interfering with HIV-1 replication.

ZFP36L2 interacts with HIV-1 transcripts via Rev binding

To determine whether ZFP36L2 requires the RRE to inhibit nuclear export, we used a gag-pol expression vector with or without RRE (Fig. 3a). In the absence of RRE, ZFP36L2 failed to inhibit cytoplasmic viral RNA accumulation, regardless of whether Rev was coexpressed (Fig. 3b,c). However, when RRE was present, ZFP36L2 restored its inhibitory effect, but only in the presence of rev (Fig. 3d,e). Under these conditions, ZFP36L2 reduced cytoplasmic gag RNA levels by ~11-fold and increased nuclear gag RNA levels by ~1.9-fold, without altering total gag RNA levels—consistent with impaired nuclear export. Proper cellular fractionation was validated using Lamin B (nuclear), GAPDH (cytoplasmic), rev, and ZFP36L2 as markers (Fig. 3c,e). Moreover, the absence of proviral DNA contamination was confirmed by RT-minus qPCR controls. These results suggest that ZFP36L2 does not directly recognize the RRE directly but instead acts through a Rev-dependent mechanism.

To investigate whether ZFP36L2 physically interacts with Rev, we first evaluated its ability to bind HIV-1 Rev versus FIV Rev, since ZFP36L2 inhibits HIV-1 but not FIV. Co-immunoprecipitation assays demonstrated that ZFP36L2 interacts with HIV-1 Rev but not FIV Rev (Supplementary Fig. 4a–c). Subsequently, we expanded this analysis to Rev

proteins from HIV-2, SIVmac239, and EIAV. ZFP36L2 was found to bind to Rev from HIV-1, HIV-2, SIVmac239, and EIAV, but not FIV (Supplementary Fig. 4d), correlating with its antiviral activity against these viruses. Notably, ZFP36L2 did not inhibit MLV or HBV, which lack a Rev homolog, further supporting a Rev-dependent mechanism. To determine whether the interaction between ZFP36L2 and Rev is RNA-mediated, we performed co-immunoprecipitation in the presence of nuclease. The interaction persisted (Fig. 3f, left and right), indicating that it is RNA-independent and likely reflects direct protein–protein binding. This was further confirmed using *in vitro* pulldown assays with recombinant His-tagged ZFP36L2 protein, which bound directly to HIV-1 and EIAV Rev, but not FIV Rev (Supplementary Fig. 4e,f). Because all ZFP36 family members exhibit some degree of anti-HIV activity, we assessed whether ZFP36 and ZFP36L1 also bind Rev. Both proteins bound HIV-1 Rev, although more weakly than ZFP36L2 (Supplementary Fig. 4g). This weaker binding reflects their relatively modest inhibitory effects on HIV-1 production compared to that of ZFP36L2 (Supplementary Fig. 1a,b), highlighting the superior affinity and functional potency of ZFP36L2 among the family members.

To determine the importance of the ZFP36L2–Rev interaction in antiviral function, we generated GFP-tagged ZFP36L2 deletion mutants (Supplementary Fig. 5a). Deletion of the C-terminal region (amino acids 446–480) abrogated binding to Rev (Supplementary Fig. 5b, left and right), severely impairing anti-HIV-1 activity (Supplementary Fig. 5c,d). In contrast, mutants that retained Rev binding maintained their antiviral activity. These findings establish that binding to Rev is essential for the ZFP36L2-mediated inhibition of HIV-1 replication. Finally, we examined the antiviral activity of ZFP36L2 orthologs from

human, mouse, rhesus macaque, and *Felis catus* against HIV-1, HIV-2, SIV, FIV, and MLV. ZFP36L2 from human, mouse, and macaque—but not from *Felis catus*—successfully inhibited HIV-1 and SIV production (Supplementary Fig. 6a,b). None of the orthologs inhibited FIV or MLV (Supplementary Fig. 6c,d). Binding assays showed that only human, mouse, and macaque ZFP36L2 bound to HIV-1 and SIV Rev (Supplementary Fig. 6e,f), while none interacted with FIV Rev (Supplementary Fig. 6g). These results account for the observed species-specific antiviral activity and support the conclusion that ZFP36L2 selectively inhibits Rev-dependent lentiviruses by binding to rev and blocking the nuclear export of RRE-containing viral transcripts.

HIV-1*rev Δ(109-116)* mutant is resistant to ZFP36L2-mediated inhibition

To further substantiate the role of Rev in ZFP36L2-mediated inhibition, we generated a panel of HIV-1 Rev deletion mutants (Δ27–50, Δ51–72, Δ73–91, Δ91–99, Δ100–108, and Δ109–116) to identify regions required for interaction with ZFP36L2. Co-immunoprecipitation assays revealed that Δ73–91 and Δ109–116 Rev mutants failed to bind ZFP36L2, despite exhibiting comparable ZFP36L2 pulldown efficiency (Supplementary Fig. 7a, left and right). To assess functional competence, we tested whether these mutants could replace wild-type Rev in rescuing Rev-defective HIV-1 production. Only the Δ109–116 mutant Rev supported virus production at levels similar to those of wild-type Rev, whereas the Δ73–91 mutant was nonfunctional (Supplementary Fig. 7b). These results suggest that the Δ109–116 mutant may retain functional activity but evades ZFP36L2 inhibition. To directly investigate this, we expressed either wild-type or Δ109–116 mutant Rev in the context of Rev-defective HIV-1 and evaluated viral

production with or without ZFP36L2. As expected, viral production was not observed without Rev (Fig. 3g). Both wild-type and Δ109–116 mutant Rev rescued HIV-1 production comparably; however, ZFP36L2 inhibited only wild-type Rev-mediated production. In contrast, ZFP36L2 had no significant effect on viral output in the presence of the Δ109–116 Rev mutant. We next examined viral RNA localization. ZFP36L2 inhibited cytoplasmic accumulation and promoted nuclear retention of viral transcripts in the presence of wild-type Rev, but not Δ109–116 mutant Rev (Fig. 3h). The fractionation efficiency was validated by assessing GAPDH and Lamin B levels. Similarly, ZFP36L2 suppressed Gag protein expression only when wild-type Rev was present (Fig. 3i), further confirming that it blocks Rev-mediated nuclear export of viral RNA.

To confirm these findings in the context of replication-competent HIV-1, we replaced the *rev* gene in the HIV-1_{NL4-3} proviral vector with the Δ109–116 mutant and assessed the effect of ZFP36L2. ZFP36L2 could no longer inhibit HIV-1*revΔ109–116* production in HeLa cells, in contrast to its potent suppression of wild-type virus (Fig. 4a). Similar resistance was observed in Jurkat T cells (Fig. 4b,c) and primary $CD4^+$ T lymphocytes (Fig. 4d,e), confirming that the Δ109–116 mutation renders HIV-1 resistant to ZFP36L2 inhibition. To evaluate whether ZFP36L2 affects the spread of HIV-1*revΔ(109-116),* we monitored replication kinetics over 8 days. Although ZFP36L2 suppressed the replication of wild-type HIV-1 in both Jurkat cells (Fig. 4f,g) and $CD4^+$ T cells (Fig. 4h,i), HIV-1*revΔ109–116* replication remained unaffected. Importantly, ZFP36L2 expression did not impair host cell proliferation (Supplementary Fig. 1c), excluding cell growth effects as a confounding variable. Notably, the HIV-1*revΔ109–116* mutant exhibited reduced replication ability compared to wild-type HIV-1, likely owing to the partial functional

deficiency of mutant Rev, as reflected by its lower Gag production in producer cells (Fig. 4a,b,d).

To investigate the molecular basis of this resistance, we assessed whether ZFP36L2 could still associate with viral RNA in the presence of mutant Rev. RNA immunoprecipitation revealed that ZFP36L2 bound to Gag transcripts in wild-type HIV-1, but not in the HIV-1*revΔ109–116* context (Supplementary Fig. 7c,d). RT-minus qPCR confirmed that these results were not due to DNA contamination. Together, these findings demonstrate that ZFP36L2 requires direct interaction with Rev to bind viral RNA and inhibit its nuclear export. The Δ109–116 Rev mutant, which cannot bind ZFP36L2, functions as an escape mutant that confers resistance to ZFP36L2-mediated inhibition.

IFN-β induces ZFP36L2 expression to inhibit HIV-1 infection

To determine whether endogenous ZFP36L2 restricts HIV-1 replication, we first evaluated its function in primary macrophages, where it is constitutively expressed. RNA interference (RNAi)-mediated *ZFP36L2* knockdown in macrophages infected with CCR5-tropic HIV-1_{AD8} resulted in significantly enhanced viral spread over a 15-day period (Supplementary Fig. 8a,b), indicating that ZFP36L2 intrinsically limits HIV-1 infection in these cells. Moreover, endogenous ZFP36L2 consistently restricted HIV-1 Gag, but not Rev, RNA nuclear export in macrophages (Supplementary Fig. 8c–e). Given that IFN-β, but not IFN-α, upregulates ZFP36L2 expression in both $CD4^+$ T cells and macrophages, we investigated whether IFN-β-mediated HIV-1 inhibition is dependent on ZFP36L2. Notably, IFN-β also induces the expression of the host restriction factor MX2. To specifically evaluate the contribution of ZFP36L2, we exploited the differential

expression kinetics of these two genes: ZFP36L2 expression peaks at 48 h posttreatment, whereas MX2 levels decline (Supplementary Fig. 2h,i). Accordingly, $CD4^+$ T cells and macrophages were treated with IFN-β for 48 h before HIV-1 infection. In $CD4^+$ T cells, ZFP36L2 knockdown markedly impaired IFN-β-mediated suppression of HIV-1 production, while IFN-α-mediated inhibition remained unaffected (Fig. 5a,b). In control cells, IFN-β reduced viral titers by 7.2- and 7.7-fold, whereas in ZFP36L2-depleted cells, suppression was reduced to only 1.3- and 1.2-fold. In contrast, IFN-α reduced HIV-1 titers to a similar extent in both control and ZFP36L2 knockdown cells (6.1- vs. 5.4-fold; 6.6- vs. 5.9-fold). Immunoblotting confirmed effective *ZFP36L2* silencing and showed that ZFP36L2 expression was induced by IFN-β but not IFN-α. Correspondingly, Gag protein levels were restored in IFN-β-treated ZFP36L2-deficient cells, but not in IFN-α-treated cells. The modest increase in viral titers following ZFP36L2 knockdown under unstimulated conditions suggests that basal ZFP36L2 partially restricts HIV-1 in $CD4^+$ T cells. Similar ZFP36L2-dependent IFN-β inhibition was observed in primary macrophages (Supplementary Fig. 8f,g). ZFP36L2 silencing impaired the ability of IFN-β—but not IFN-α—to suppress HIV-1. Because of the higher basal ZFP36L2 levels in macrophages (Supplementary Fig. 2a), knockdown alone increased viral replication, even without IFN stimulation.

MX2 primarily acts during early replication by blocking viral core translocation from the cytoplasm to the nucleus, whereas ZFP36L2 exerts inhibitory effects at later stages. To minimize the antiviral contribution of MX2, we electroporated proviral $HIV\text{-}1_{NL4\text{-}3.Luc.\ R\text{-}.E\text{-}}$ vectors into $CD4^+$ T cells in the presence or absence of IFNs. In these transfected cells, HIV-1 completes only the late stages of replication, during which MX2 has no effect,

because it acts early in the viral life cycle. This approach allowed us to specifically assess the role of ZFP36L2. Under these conditions, ZFP36L2 knockdown continued to impair IFN-β-mediated suppression of HIV-1 titers in $CD4^+$ T cells (Supplementary Fig. 9a,b), suggesting that IFN-β induces ZFP36L2 to function in producer cells, where it inhibits HIV-1 production.

To further confirm the role of ZFP36L2 in IFN-β-mediated HIV-1 inhibition, we evaluated infections with wild-type or *revΔ(109-116)* mutant HIV-1, which is resistant to ZFP36L2, in $CD4^+$ T cells treated with or without IFNs (Fig. 5c,d). IFN-α and IFN-β reduced wild-type HIV-1 titers by 15.2- and 12.2-fold (Fig. 5c) and 11.3- and 9.03-fold (Fig. 5d), respectively. In contrast, *revΔ(109-116)* mutant HIV-1 titers were reduced by 13.1- and 10.7-fold with IFN-α, but only by 1.45- and 2.1-fold with IFN-β. This suggests that the mutant is resistant to ZFP36L2-mediated IFN-β inhibition, but remains sensitive to IFN-α, likely because of mechanisms independent of ZFP36L2. To confirm this finding, we knocked down ZFP36L2 in HIV-1-infected $CD4^+$ T cells and assessed the effects of IFN stimulation. In wild-type HIV-1 infections, ZFP36L2 knockdown reduced IFN-β-mediated inhibition from 7.2-fold to 1.3-fold (Fig. 5e), confirming the role of ZFP36L2 in this suppression. However, IFN-α inhibition remained unchanged (6.1- vs. 5.4-fold). In *revΔ(109-116)* mutant HIV-1 infections, IFN-β conferred only a modest 1.6-fold reduction in viral titers, which was unaffected by ZFP36L2 knockdown (1.6- vs. 1.2-fold), indicating that IFN-β acts via ZFP36L2-independent pathways. Immunoblotting confirmed successful ZFP36L2 depletion and revealed that Gag protein levels were restored in wild-type—but not *revΔ(109-116)*—infected cells treated with IFN-β (Fig. 5f). Similar results were observed in primary macrophages transfected with proviral vectors encoding wild-

type or *revΔ(109-116)* mutant HIV-1, with or without IFN treatment (Supplementary Fig. 9c,d). Importantly, this proviral transfection approach reduces the influence of endogenous MX2, which acts in the early viral life cycle stage but has no effect in producer cells. Consistently, ZFP36L2 depletion impaired IFN-β-mediated suppression of wild-type HIV-1, but not *revΔ(109-116)* HIV-1 titers. Notably, macrophages expressed higher basal levels of ZFP36L2 than $CD4^+$ T cells even without IFN stimulation. Overall, these findings demonstrate that IFN-β induces ZFP36L2 to inhibit HIV-1 replication in both $CD4^+$ T cells and macrophages, and that this effect is circumvented by the *revΔ(109-116)* mutant, which is resistant to ZFP36L2-mediated inhibition.

IFN-β induces ZFP36L2 expression to inhibit HIV-1 spread in $CD4^+$ T cells from HIV-1-infected individuals *ex vivo*

To investigate the role of ZFP36L2 in HIV-1 infection *in vivo*, we first analyzed ZFP36L2 mRNA levels in $CD4^+$ T cells from three groups: ART-naive HIV-1-infected individuals (Supplementary Table 1), ART-treated individuals with suppressed viral loads (<50 copies/mL; Supplementary Table 2), and healthy donors. ZFP36L2 expression was comparable between healthy donors and ART-treated individuals but was significantly increased in $CD4^+$ T cells from ART-naive individuals (Fig. 6a). This upregulation may result from endogenous IFN or cytokine stimulation during active HIV-1 infection. To further assess the anti-HIV-1 function of ZFP36L2 *in vivo*, we analyzed correlations between ZFP36L2 expression in $CD4^+$ T cells and its clinical parameters. ZFP36L2 transcript levels were inversely correlated with plasma HIV-1 RNA levels (Fig. 6b). This correlation may not be specific, as ZFP36L2 is an IFN-stimulated gene, and similar

correlations may also be observed for other IFN-induced genes. Moreover, ZFP36L2 expression was inversely correlated with $CD4^+$ T cell counts (Fig. 6c); however, it exhibited no correlation with the $CD4^+/CD8^+$ T cell ratio (Fig. 6d), suggesting that ZFP36L2 activity is closely associated with HIV-1-infected $CD4^+$ T cells and may contribute to $CD4^+$ T cell depletion.

To directly assess the antiviral function of ZFP36L2 *ex vivo*, we isolated total $CD4^+$ T cells from ART-naive and ART-treated HIV-1-infected individuals with suppressed viral loads (<50 copies/mL; their backgrounds in Supplementary Table 3). Following stimulation for lentiviral transduction, cells were transduced with either a wild-type or Δ446–480 mutant ZFP36L2-GFP expression vector or a GFP-only control vector and subsequently subjected to puromycin selection (Fig. 6e). Exogenous ZFP36L2 expression did not affect $CD4^+$ T cell proliferation (Fig. 6f), however, it significantly inhibited HIV-1 spread compared to the Δ446–480 mutant ZFP36L2-GFP or the GFP-only control (Fig. 6g,h). These results demonstrate that ZFP36L2 overexpression suppresses HIV-1 replication in $CD4^+$ T cells *ex vivo* and highlight its potential as a gene therapy candidate. We next investigated whether IFN-β could induce ZFP36L2 to inhibit HIV-1 replication in $CD4^+$ T cells *ex vivo*. $CD4^+$ T cells isolated from ART-naive HIV-1-infected individuals (Supplementary Table 4) were transduced with lentiviral vectors encoding either control or ZFP36L2-specific shRNA in the presence or absence of IFN-β. ZFP36L2 knockdown significantly impaired the ability of IFN-β to suppress HIV-1 production (Fig. 6i). Moreover, virion production was inversely correlated with ZFP36L2 expression levels (Fig. 6j). Cell proliferation was unaffected by ZFP36L2 knockdown (Fig. 6k), indicating that the reduction in IFN-β-mediated suppression was due to ZFP36L2

depletion. Similar results were observed in CD4$^+$ T cells obtained from ART-treated HIV-1-infected individuals: ZFP36L2 knockdown impaired IFN-β-mediated inhibition of HIV-1 spread *ex vivo* (Fig. 6l–n). Taken together, these findings demonstrate that IFN-β induces ZFP36L2 expression to impede HIV-1 replication in CD4$^+$ T cells *ex vivo*, validating the physiological relevance of this antiviral pathway in human HIV-1 infection.

Discussion

The innate immune response serves as the body's first line of defense against HIV-1 infection. Upon viral recognition, it triggers the production of IFN-Is, a family of antiviral cytokines that includes IFN-α and IFN-β [36]. IFN-Is signal through the IFN-I receptor to induce the expression of several ISGs, which collectively orchestrate a broad antiviral defense. IFN-α, comprising 12 subtypes, plays a key role in controlling HIV-1 and is elevated in the plasma of infected individuals [37, 38]. Interestingly, IFN-β induces a broader spectrum of ISGs than individual IFN-α subtypes and, unlike IFN-α, is specifically upregulated in the gut during chronic HIV-1 infection [39]. These observations suggest distinct yet complementary roles for IFN-α and IFN-β in antiviral immunity and HIV-1 pathogenesis. In this study, we found that IFN-β selectively induces the expression of ZFP36L2, a nuclear RNA-binding protein, in primary CD4$^+$ T cells and macrophages. ZFP36L2 belongs to the CCCH-type zinc finger RNA-binding protein family, which comprises ZFP36 and ZFP36L1 [24, 25]. These proteins contain two conserved zinc finger domains and typically function by binding to AU-rich elements in mRNAs, promoting transcript destabilization. Notably, IFN-α did not induce ZFP36L2 expression in either

CD4$^+$ T cells or macrophages. Among the ZFP36 family members, only ZFP36L2 was robustly induced by IFN-β, identifying it as an IFN-β-responsive factor.

Given that MX2 is a well-established IFN-induced restriction factor against HIV-1, we compared the expression kinetics of MX2 and ZFP36L2 following IFN stimulation. MX2 peaked at 12 h and declined thereafter, whereas ZFP36L2 expression gradually increased, peaking at 48 h. Accordingly, we pretreated primary CD4$^+$ T cells and macrophages with IFN-β for 48 h before HIV-1 infection for maximum ZFP36L2 expression and minimal MX2 levels. Under these conditions, ZFP36L2 silencing significantly impaired IFN-β-mediated HIV-1 suppression in both cell types. However, ZFP36L2 depletion had no effect on the antiviral activity of IFN-α. To further exclude potential MX2-associated effects, we transfected CD4$^+$ T cells and macrophages with HIV-1 proviral vectors, thereby circumventing the influence of MX2, as it acts during the early stage of viral replication and has no effect on producer cells. Even under these conditions, ZFP36L2 knockdown impaired IFN-β-mediated suppression of HIV-1, confirming its role as an antiviral effector. These findings suggest that, in addition to MX2, ZFP36L2 is an IFN-β-induced antiviral effector in CD4$^+$ T cells and macrophages. In our experimental systems, ZFP36L2 knockdown reverses nearly ~80% of IFN-β–mediated HIV-1 suppression. This pronounced effect stems from our tailored approaches—proviral DNA delivery and timed infections—which minimize the activity of early-phase inhibitors like MX2, thereby isolating the late replication phase where ZFP36L2 acts. Thus, ZFP36L2 emerges as a predominant, non-redundant effector of IFN-β against post-integration steps. This specialized role does not negate the broader importance of other ISGs in vivo; the residual suppression likely involves other late-acting factors. Future in

vivo studies will be needed to quantify ZFP36L2's contribution within the full ISG network across the entire viral life cycle. Additionally, among the ZFP36 family members, ZFP36 and ZFP36L1 revealed only modest anti-HIV-1 effects, further highlighting ZFP36L2 as the primary antiviral member induced by IFN-β. However, whether ZFP36 and ZFP36L1 use similar antiviral mechanisms needs further investigation.

We next assessed how ZFP36L2 inhibits HIV-1 during the late phase of viral replication. ZFP36L2 overexpression significantly decreased HIV-1 production across various host cells—including 293T, HeLa, Jurkat, and $CD4^+$ T cells—as measured by viral titers. Intracellular Gag and Env protein levels were substantially decreased in the presence of ZFP36L2, whereas Nef levels remained unaffected. Because Gag and Env, but not Nef, transcripts contain the RRE, we hypothesized that ZFP36L2 targets RRE-containing transcripts. The fractionation of nuclear and cytoplasmic RNA revealed that the cytoplasmic levels of *gag*, *vpu*/*env*, *vif*, and *vpr* were markedly reduced, whereas their nuclear levels were elevated in ZFP36L2-expressing cells. In contrast, the total RNA levels of *gag*, *vpu*/*env*, *vif*, *vpr*, *nef*, and *tat* remained unchanged, suggesting that ZFP36L2 specifically inhibits the nuclear export of RRE-containing transcripts. In accordance with this, ZFP36L2 selectively inhibited the cytoplasmic export of RRE-containing gag transcripts only in the presence of Rev. However, ZFP36L2 had no effect on these transcripts in the absence of Rev, indicating that its antiviral function is Rev-dependent. Moreover, co-immunoprecipitation (CoIP) assays confirmed that ZFP36L2 directly binds Rev in uninfected cells. Interestingly, ZFP36 and ZFP36L1 demonstrated much weaker interactions with Rev, reflecting their reduced antiviral activity. Future work is required to determine where ZFP36L2 engages Rev within the nucleus and whether

ZFP36L2 interferes with the Rev–Crm1–Ran-GTP export machinery, thereby affecting export of Rev-dependent cargos.

To further examine this Rev-dependence, we assessed whether ZFP36L2 could inhibit other retroviruses. ZFP36L2 significantly inhibited Rev-encoding HIV-2, SIV_{mac239}, and EIAV. Moreover, CoIP assays confirmed that ZFP36L2 binds SIV_{mac239} and EIAV Rev. In contrast, ZFP36L2 had no effect on FIV, MLV, or HBV. Although FIV encodes a Rev protein, ZFP36L2 did not bind FIV Rev, thereby failing to inhibit FIV replication. Since MLV and HBV lack Rev proteins, the absence of ZFP36L2-mediated inhibition is expected. Furthermore, using purified recombinant proteins, we confirmed that ZFP36L2 binds directly to HIV-1, HIV-2, and SIVmac239 Rev, but not FIV Rev. Interestingly, although the amino acid sequence of FIV Rev is distinct from those of HIV-1, HIV-2, and SIV_{mac239}, and the EIAV Rev sequence is also highly divergent—yet ZFP36L2 binds EIAV Rev. This suggests that ZFP36L2 recognition by Rev is more dependent on the three-dimensional structure than on the primary sequence. We also assessed ZFP36L2 orthologs and found that human, mouse, and rhesus macaque ZFP36L2 inhibited HIV-1 and SIV_{mac239}, whereas *Felis catus* ZFP36L2 did not. None of the orthologs—including feline ZFP36L2—affected FIV or MLV, nor did any bind FIV Rev, further supporting the structural specificity of the Rev–ZFP36L2 interaction.

Rev mutants that are resistant to ZFP36L2 were identified using CoIP assays. Two deletion mutants—Δ73–91 and Δ109–116—were identified that failed to bind ZFP36L2. Of these, only Δ109–116 retained the ability to support viral replication. As expected, ZFP36L2 failed to inhibit the *rev∆(109-116)* mutant virus while still effectively suppressing

wild-type HIV-1. In 8-day spreading infections, ZFP36L2 had no inhibitory effect on the *revΔ(109-116)* mutant virus in Jurkat or primary $CD4^+$ T cells. Although the mutant produced slightly lower titers than the wild-type rev (likely owing to the deletion), this does not alter our conclusion that ZFP36L2 requires interaction with Rev to exert its antiviral effect. Consistently, IFN-β strongly suppressed wild-type HIV-1 but only mildly inhibited the *revΔ(109-116)* mutant in $CD4^+$ T cells and macrophages. In contrast, IFN-α inhibited both viruses similarly. Moreover, ZFP36L2 knockdown impaired IFN-β-mediated suppression of wild-type HIV-1; however, it had no effect on the *revΔ(109-116)* mutant. Similarly, ZFP36L2 depletion had no effect on IFN-α-mediated suppression. All experiments used a 48-h IFN-β pretreatment to minimize endogenous MX2 effects. Moreover, consistent results were observed in HIV-1-transfected producer cells carrying proviral vectors, where MX2 had no effect on HIV-1 titers. These findings suggest that ZFP36L2 functions as an effector of IFN-β-mediated antiviral activity against HIV-1, acting as an additional factor alongside MX2. An important future question is whether Rev sequences from HIV-1–infected individuals contain natural polymorphisms that allow escape from ZFP36L2, and whether such polymorphisms correlate with differences in disease progression. Determining whether the 109–116 region of Rev varies across clinical isolates will be essential for understanding potential ZFP36L2-driven selection.

Finally, we assessed the *in vivo* relevance of ZFP36L2. ZFP36L2 RNA levels were higher in $CD4^+$ T cells obtained from ART-naive individuals than in those from ART-treated individuals, likely reflecting IFN stimulation. Because IFN-β was undetectable in peripheral blood mononuclear cells (PBMCs) or plasma, further investigation is needed

to understand whether ZFP36L2 expression is directly induced by IFN-β *in vivo*. ZFP36L2 transcript levels were inversely correlated with HIV-1 viral load, though this relationship may not be specific, as ZFP36L2 is an interferon-stimulated gene and similar correlations may occur for other ISGs. Moreover, ZFP36L2 levels were inversely correlated with $CD4^+$ T cell counts, likely owing to IFN signaling in untreated HIV-1-infected individuals. To validate these observations, ZFP36L2 was knocked down in $CD4^+$ T cells isolated from 17 ART-naive and 23 ART-treated individuals in the presence or absence of IFN-β. In all cases, ZFP36L2 depletion could significantly reduce the antiviral effect of IFN-β *ex vivo*. In conclusion, we identify ZFP36L2 as an IFN-β–induced antiviral effector that restricts HIV-1 by directly binding to the Rev protein and blocking the nuclear export of viral transcripts. This mechanism operates alongside, but independently of early-phase factors such as MX2, thereby expanding our understanding of the temporal layering within the interferon response. Although the generalizability of findings from some primary-cell experiments (n = 3) warrants confirmation in larger cohorts, our work establishes a Rev-dependent restriction node. Future studies should investigate natural Rev polymorphisms that may confer viral escape in patients and define the structural basis of the ZFP36L2–Rev interaction, which may inform host-directed therapeutic strategies against HIV-1.

METHODS

Ethics statement

This study (Protocol No. 2021-328-2 on June 24 2021) is approved by the Research and Ethics Committee of The First Hospital of China Medical University. All blood samples were obtained from healthy donors following National Health and Medical Research Council guidelines. In addition, informed consent was obtained from each healthy donor prior to the study.

Biosafety statement

All experiments involving infectious materials were conducted in a certified Biosafety Level 3 (BSL-3) facility in accordance with institutional and national guidelines. These protocols ensured the safe conduct of research and the protection of personnel and the environment. This study advances the fundamental understanding of host antiviral defenses and may have potential therapeutic implications. With regard to potential Dual-Use Research of Concern (DURC) associated with the HIV-1 *RevΔ(109–116)* mutant described in this study, this mutant virus was generated solely for mechanistic investigations and was examined exclusively in controlled in vitro and ex vivo experimental systems. Importantly, the mutant does not exhibit enhanced replication capacity or pathogenicity compared with the wild-type virus; rather, it demonstrates reduced replication capacity relative to wild-type HIV-1. All experiments were conducted in strict compliance with institutional biosafety regulations and were reviewed and approved by the appropriate biosafety oversight committees.

HIV-1-infected individuals

ART-naive or treated patients with viral loads of <50 copies/mL and untreated HIV-1$^+$ patients were enrolled in this study. Peripheral blood mononuclear cells (PBMCs) from patients were prepared using Ficoll-Hypaque density gradient centrifugation. CD4$^+$ T cells were isolated from PBMCs by negative selection using a human CD4$^+$ T-cell enrichment cocktail (Stem Cell Technologies). Ethical approval was obtained from the Research and Ethics Committee of The First Hospital of China Medical University (approval no. 2021-328-2 on June 24 2021), and written informed consent for participation was obtained from all participants.

Cells and culture reagents

HeLa, 293T, TZM-bl, and Jurkat cells were cultured and maintained in Dulbecco's modified Eagle's medium (Gibco) or RPMI-1640 medium (Gibco). Both media were supplemented with 10% fetal bovine serum (FBS, Gibco), 100 U/mL penicillin, and 100 mg/mL streptomycin. Plasmids were transfected into 293T cells using Lipofectamine 2000 (Invitrogen), in accordance with the manufacturer's instructions. PBMCs obtained from healthy blood donors were purified using Ficoll-Hypaque gradient centrifugation. CD4$^+$ T cells or monocytes were isolated from PBMCs via negative selection using human CD4$^+$ T cells or a CD14$^+$ enrichment cocktail (StemCell Technologies). To stimulate CD4$^+$ T cells, CD3/CD28 activator magnetic beads (Invitrogen) were added to the culture medium along with IL-2 (50 U/mL) (Biomol) for 2 days, in accordance with the manufacturer's instructions. The isolation and culture of monocytes, monocyte-derived macrophages (MDMs), and monocyte-derived dendritic cells (MDDCs) were performed [40, 41]: MDMs were produced by stimulating monocytes with 10 ng/mL recombinant human granulocyte-

macrophage colony-stimulating factor (GM-CSF, R&D) and 50 ng/mL recombinant human macrophage colony-stimulating factor (M-CSF, R&D) for 7 days. MDDCs were generated by incubating CD14-purified monocytes in Iscove's modified Dulbecco's medium (Gibco) supplemented with 10% FBS, 2 mM L-glutamine, 100 IU/mL penicillin, 100 mg/mL streptomycin, 10 mM HEPES, 1% nonessential amino acids, 1 mM sodium pyruvate, 10 ng/mL GM-CSF, and 50 ng/mL IL-4 (Miltenyi Biotec). On Day 4, two-thirds of the culture medium was replaced with fresh medium containing GM-CSF and IL-4. Immature MDDCs were harvested on Day 6 and used for experiments.

Reagents

IFN-α (Cat# 1103-IF-0101), IFN-β1a (Cat# 8499-IF-010), IFN-γ (Cat# 285-IF-100), and IL-2 (Cat# 202-IL) were purchased from R&D. PHA (Cat# 11249738001) was obtained from Roche.

Plasmids

The ZFP36, ZFP36L1, and ZFP36L2 expression vectors were purchased from OriGene, and their open reading frames were *de novo* cloned into the pCMV-3Tag-2A (Addgene) vector. Luciferase-expressing Env-defective HIV-$1_{NL4\text{-}3.Luc.\ R\text{-}E\text{-}}$, SIV_{mac239}-luc, HIV-2_{Rod}-luc, and MLV-luc were provided by Dr. Guangxia Gao [42]. HIV-1 proviral NL4-3, BaL, and 89.6 vectors were obtained through the National Institutes of Health AIDS Reagent Program. The HIV-1 proviral vectors of pNL-AD8 were gifted by Dr. Eric Freed. The microRNA-adapted shRNA for ZFP36L2 (Cat#RHS4430-200267269) or control (Cat# RHS4346)

was purchased from Dharmacon, the mature antisense shRNA for ZFP36L2 as 5'-TGCACAAGAAGTCGACATC-3'.

RNA interference in Jurkat T cells, CD4$^+$ T cells, and MDMs

Gene silencing of *ZFP36L2* was performed using a microRNA-adapted shRNA targeting the open reading frame (Cat# RHS4430-200267269; Dharmacon). A non-targeting shRNA (Cat# RHS4346; Dharmacon) served as the control. Jurkat T cells, pre-activated CD4$^+$ T cells (stimulated with CD3/CD28 and IL-2), and MDMs were transduced with the shRNA-expressing lentivirus [40, 41]: at 48 h post-transduction, cells were selected with puromycin for an additional 48 hours. For viral infection, the transduced Jurkat T cells and CD4+ T cells were challenged with replication-competent wild-type HIV-1_{NL4-3} or an isogenic Rev (Δ109-116) mutant at a comparable multiplicity of infection (MOI) for 6 hours. Of note, primary CD4$^+$ T cells derived from patients were exempt from this infection step. The cells were then washed twice with pre-cooled phosphate-buffered saline (PBS) to remove residual virus and returned to culture. MDMs were similarly infected with HIV-1_{AD8}. Culture supernatants were harvested at the indicated time points post-infection. Viral production was quantified by measuring HIV-1 p24 levels using a commercial ELISA kit (ABL) and/or by determining infectious titer using TZM-bl reporter cells, followed by measurement of luciferase activity (Promega). Additionally, the proliferation of transduced Jurkat T cells and CD4+ T cells was assessed using the CellTrace Cell Proliferation Kit (Invitrogen), according to the manufacturer's instructions.

Electroporation of Jurkat T Cells and Primary CD4$^+$ T Cells

Jurkat T cells and primary $CD4^+$ T cells activated with CD3/CD28 Dynabeads were co-electroporated with either a ZFP36L2 expression plasmid or a mock control plasmid, together with one of the following proviral vectors: NL4-3.Luc.R^-E^-, NL4-3, or NL4-3*rev Δ(109–116)*. All transfections were performed using the Lonza 4D-Nucleofector™ System with the 4D-Nucleofector™ X Unit. For Jurkat cells, the SE Cell Line 4D-Nucleofector™ X Kit (Lonza, Cat# V4XC-3024) and program CL-120 were used. For primary $CD4^+$ T cells, the P3 Primary Cell 4D-Nucleofector™ X Kit (Lonza, Cat# V4XP-3024) was used, with program EO-115 for activated cells [40, 41].

Cytoplasmic and nuclear RNA purification

Cytoplasmic and nuclear RNAs were isolated using a Cytoplasmic & Nuclear RNA Purification Kit (Norgen; Cat# 37400) according to the manufacturer's protocol. Briefly, cells were lysed using the provided cytoplasmic lysis buffer, followed by centrifugation for the separation of cytoplasmic (supernatant) and nuclear (pellet) fractions. The cytoplasmic RNA was then purified from the supernatant using RNA purification columns, whereas nuclear RNA was extracted from the pellet after disruption with nuclear lysis buffer. Both RNA fractions were treated with DNase I to eliminate genomic DNA contamination. RNA concentration and purity were assessed using a NanoDrop spectrophotometer (Thermo Fisher Scientific), and gene expression levels were analyzed by RT-PCR.

Enzyme-linked immunosorbent assay

ELISA was used to measure p24 protein in the culture supernatants (ABL Corporation) according to the manufacturer's instructions. Test samples were mixed with disruption buffer to inactivate the virus and release HIV-1 p24 into solution for detection. Microtiter wells of a 96-well plate were coated with two murine monoclonal antibodies specific for distinct epitopes on HIV-1 p24. HIV-1 p24 standard solutions or tissue culture test samples were added to the wells, allowing p24 to form immune complexes with the plate-bound antibodies. Unbound materials were then removed by thorough washing. A conjugate solution, containing peroxidase-conjugated human anti-p24 polyclonal antibodies then added to bind the captured HIV-1 p24. After washing the wells to remove the unbound conjugated antibodies, a peroxidase substrate was added. The enzyme–substrate reaction produces a blue color change, which turns yellow upon addition of stop solution. Absorbance was measured at 450 nm. A linear relationship was observed between absorbance and HIV-1 p24 concentration, and sample concentrations were determined by linear regression analysis using the standard curve.

Luciferase detection assay

Luciferase activity was quantified as relative luminescence units (RLUs) in cell lysates using the manufacturer's instructions (Promega). The TZM-bl indicator cell line was used to quantify HIV-1 infectivity, with luciferase serving as a reporter. Background luminescence from uninfected TZM-bl cells was subtracted from each data point.

Measurement of viral infectivity

HIV-1 p24 levels in culture supernatants were measured using an ELISA (ABL Corporation). To assess viral infectivity, culture supernatants were used to infect TZM-bl reporter cells. Following infection, luciferase activity in cell lysates was measured in RLUs (Promega). Background luminescence from uninfected TZM-bl cells was subtracted from each data point.

HBV nucleocapsid-associated DNA purification

Briefly, secreted HBV particles were purified from culture supernatants using PEG8000 (30% in NaCl) precipitation. The purified relaxed circular DNA from the nucleocapsid-associated DNA was obtained after the following treatments: DNase I digestion to eliminate transfected plasmids, proteinase K and SDS digestion, phenol–chloroform extraction, and isopropanol precipitation. HBV DNA was quantified using qPCR analysis using the primer set 5′-GAATTGATGACTCTAGCTACCTG-3' and 5′-GAAACCACAATAGTTGCCTGATC-3′ [43] .

Southern Blotting

The primer sequences for various spliced forms of HIV mRNA and the probes used were previously described [44]. Briefly, cDNAs corresponding to unspliced and singly spliced HIV-1 mRNAs were amplified using primers FP and RP1, while cDNAs for multiply spliced HIV-1 mRNAs were amplified using primers FP and RP2. PCR products were separated on a 1.2% agarose gel, followed by Southern blotting. PCR products amplified from NL4-3.Luc.R-.E- using primers HIV6078F and HIV6621R were used as templates to generate probes for detecting RT-PCR products derived from unspliced and singly spliced mRNAs.

Similarly, PCR products amplified using primers HIV8396F and HIV8776R served as templates for probes targeting multiply spliced mRNA RT-PCR products. Probes were labeled with biotin-14-dCTP by random priming (DNA Labeling System, Thermo). The quantity of PCR products was analyzed using the Chemiluminescent Nucleic Acid Detection Module (Thermo).

Primer sequences:

FP: 5′-AGTAAAGCCAGAGGAGATCTCTCG-3′

RP1: 5′-ATTGGTATTAGTATCATTCTTCAAATC-3′

RP2: 5′-GCCACCCATCTTATAGCAAAATCC-3′

HIV6078F: 5′-GTAGCAATAGTAGCATTAGTAGTAGC-3′

HIV6621R: 5′-ATTGGTATTAGTATCATTCTTCAAATC-3′

HIV8396F: 5′-ACCCGACAGGCCCGAAGGAATAG-3′

HIV8776R: 5′-GCCACCCATCTTATAGCAAAATCC-3′

Co-immunoprecipitation

293T or HeLa cells (5.0×10^6) were lysed using IP lysis buffer (50 mM Tris–HCl, pH 7.2, 50 mM NaCl, 1% NP-40, 1 mM EDTA, 2% glycerol, and 1× protease inhibitor cocktail). The lysates were incubated on ice for 30 min and then centrifuged at 12,000 rpm and 4°C for 10 min. The supernatants were then transferred to fresh tubes, and the pellets were mixed with cold IP lysis buffer prior to sonication, followed by a second round of centrifugation at 12,000 ×*g* and 4°C for 10 min. The supernatants obtained from the two extraction steps were pooled and incubated with mixed protein A and G Dynabeads

(Invitrogen) pretreated overnight with antibodies at 4°C. The IP products were washed with cold IP and PBST buffers 5–10 times (500 µL per wash).

Cytotoxicity assays

The culture supernatants of lentiviral-transduced or untransduced MDMs were collected to assess LDH release. Cytotoxicity was quantified colorimetrically using the Pierce LDH Cytotoxicity Kit (Thermo Fisher Scientific), with LDH activity measured by subtracting $A_{490\ nm}$ from $A_{680\ nm}$. Lysis control wells were treated with 10× lysis buffer for 1 h. The cytotoxicity percentage was calculated using a previously described formula [45]:

$$LDH = (LDH_{lenti\text{-}MDM} - LDH_{MDM}) / (LDH_{Maximum} - LDH_{MDM}) \times 100\%$$

where $LDH_{lenti\text{-}MDM}$ or LDH_{MDM} is the amount of LDH activity in the supernatants of lentiviral-treated and untreated cells, respectively, and $LDH_{Maximum}$ represents the activity in the supernatant of the lysis control. LDH activity present in cell-free culture medium was subtracted from all values before normalization.

Expression and purification of recombinant proteins

All recombinant GST-proteins were expressed in BL21(DE3) cells at 37°C and induced with 1 mM isopropyl β-D-1-thiogalactopyranoside for 3.5 h, as described previously[46]: Cell pellets were lysed by ultrasonication in lysis buffer, clarified by centrifugation at 12,000 ×*g* for 30 min, and purified by GST-tagged Purification Resin (GST-tag Protein Purification Kit, Beyotime Biotechnology, Beijing, China). All His-ZFP36L2 recombinant proteins were expressed in Rosetta 2 cells and purified on a HisTrap HP column using a 250 mM

imidazole gradient (His-tag Protein Purification Kit, Beyotime Biotechnology). All recombinant proteins were resolved by SDS-polyacrylamide gel electrophoresis (PAGE) and analyzed using western blotting with specific antibodies [mouse monoclonal anti-His (Cell Signaling) and anti-GST (Abcam)].

Subcellular protein fractionation

Nuclear and cytoplasmic protein extracts were isolated using Cell Lysis Buffer (Cell Signaling Technology; Cat# 9803), following the manufacturer's protocol with minor modifications. Briefly, harvested cells were washed with ice-cold PBS and lysed in 1× Cell Lysis Buffer supplemented with protease and phosphatase inhibitor (Thermo Fisher Scientific; Cat# 78442) for 5 min on ice. Lysates were centrifuged at 14,000 ×*g* and 4°C for 10 min, and the supernatant (cytoplasmic fraction) was collected. The remaining pellet (nuclear fraction) was resuspended in 1× Cell Lysis Buffer, followed by sonication (30 sec, 20% amplitude, on ice) to disrupt nuclear membranes. After centrifugation (14,000 ×*g*, 10 min, 4°C), the supernatant (nuclear protein extract) was collected. Protein concentrations were quantified using a BCA assay (Pierce™; Cat# 23225). Protein expression was assessed by western blotting, and GAPDH or Lamin B expression was detected separately as cytoplasmic or nuclear positive controls.

Western blotting and immunoblotting

Western blotting was performed using a standard method to detect cellular proteins. The following antibodies were used: mouse monoclonal anti-ZFP36L2 (1:500, Santa Cruz, Cat# sc-365908), rabbit anti-Lamin B (1:2500, Abcam, Cat# ab16078), mouse anti-nef

(1:500, Abcam, Cat# ab42355), Mouse anti-GAPDH (1:1000, ZSGB-BIO, Cat# TA-08), mouse monoclonal anti-FLAG (1:1000, SIGMA, Cat# F1804), mouse anti-His (1:1000, ZSGB-BIO, Cat# TA-02), mouse anti-GST (1:1000, Abcam, Cat# ab92), mouse anti-GFP (1:2500, Abmart, Cat# M20004), rabbit polyclonal anti-p24 (1:1000, Abcam, Cat# ab63913), mouse IgG-HRP (1:5000, Abcam, Cat# ab6789), rabbit IgG-HRP (1:5000, Abcam, Cat# ab6721), TrueBlot® ULTRA Anti-Mouse IgG HRP (1:1000, Rockland, Cat# 18-8817-33), and mouse IgG isotype control (1:1000, Abcam, Cat# 188776).

qPCR

Total RNA was extracted from cells using TRIzol reagent (Invitrogen), in accordance with the manufacturer's instructions. The obtained RNA was dissolved in 100 µL of DPEC-H_2O, and 1 µg of the purified RNA was treated with DNase I (amplification grade, Invitrogen) for 10–15 min at room temperature to remove residual genomic DNA. RNA was immediately primed with oligo-dT and reverse transcribed using Superscript III Reverse Transcriptase (Invitrogen). Real-time PCR was performed using the $\Delta\Delta$CT method, with gene expression levels normalized to GAPDH as the internal control. The primers used in this study are listed in Supplementary Table 6.

Statistical analysis

Statistical analyses were performed using GraphPad Prism software (version 8.0.1). Continuous data are presented as the mean ± standard deviation (SD), unless otherwise indicated. Comparisons between two independent groups were performed using an unpaired, two-tailed Student's t-test. Comparisons among three or more independent

groups under a single experimental factor were conducted using one-way analysis of variance (ANOVA), followed by Tukey's post hoc test for multiple comparisons, unless otherwise specified. For analyses involving two independent variables, two-way ANOVA was used to assess main effects and interactions. When appropriate, pairwise comparisons were performed using Šidák's multiple-comparisons test to control the family-wise error rate. A p value < 0.05 was considered statistically significant for all analyses.

Data availability

Data supporting the findings of this study are available within the article and its Supplementary Information files. Source data are provided in this paper.

References

1. Doyle, T., Goujon, C. & Malim, M.H. HIV-1 and interferons: who's interfering with whom? *Nat Rev Microbiol* 13, 403-413 (2015).
2. Schneider, W.M., Chevillotte, M.D. & Rice, C.M. Interferon-stimulated genes: a complex web of host defenses. *Annu Rev Immunol* 32, 513-545 (2014).
3. Bitzegeio, J., Sampias, M., Bieniasz, P.D. & Hatziioannou, T. Adaptation to the interferon-induced antiviral state by human and simian immunodeficiency viruses. *J Virol* 87, 3549-3560 (2013).
4. Goujon, C. & Malim, M.H. Characterization of the alpha interferon-induced postentry block to HIV-1 infection in primary human macrophages and T cells. *J Virol* 84, 9254-9266 (2010).
5. Meylan, P.R., Guatelli, J.C., Munis, J.R., Richman, D.D. & Kornbluth, R.S. Mechanisms for the inhibition of HIV replication by interferons-alpha, -beta, and -gamma in primary human macrophages. *Virology* 193, 138-148 (1993).
6. Pillai, S.K. et al. Role of retroviral restriction factors in the interferon-alpha-mediated suppression of HIV-1 in vivo. *Proc Natl Acad Sci U S A* 109, 3035-3040 (2012).

7. Schoggins, J.W. et al. A diverse range of gene products are effectors of the type I interferon antiviral response. *Nature* 472, 481-485 (2011).

8. Kane, M. et al. MX2 is an interferon-induced inhibitor of HIV-1 infection. *Nature.* 502, 563-566 (2013).

9. Goujon, C. et al. Human MX2 is an interferon-induced post-entry inhibitor of HIV-1 infection. *Nature* 24, 559-562 (2013).

10. Jakobsen, M.R. et al. IFI16 senses DNA forms of the lentiviral replication cycle and controls HIV-1 replication. *Proc Natl Acad Sci U S A* 110, E4571-4580 (2013).

11. Ma, F. et al. Positive feedback regulation of type I IFN production by the IFN-inducible DNA sensor cGAS. *J Immunol* 194, 1545-1554 (2015).

12. Lahaye, X. et al. The capsids of HIV-1 and HIV-2 determine immune detection of the viral cDNA by the innate sensor cGAS in dendritic cells. *Immunity* 39, 1132-1142 (2013).

13. Gao, D. et al. Cyclic GMP-AMP synthase is an innate immune sensor of HIV and other retroviruses. *Science* 341, 903-906 (2013).

14. Foster, T.L. et al. Resistance of Transmitted Founder HIV-1 to IFITM-Mediated Restriction. *Cell Host Microbe* 20, 429-442 (2016).

15. Sheehy, A., Gaddis, N., Choi, J. & Malim, M. Isolation of a human gene that inhibits HIV-1 infection and is suppressed by the viral Vif protein. *Nature.* 418, 646-650 (2002).

16. Neil, S., Zang, T. & Bieniasz, P. Tetherin inhibits retrovirus release and is antagonized by HIV-1 Vpu. *Nature* 451, 425-430 (2008).

17. Wang, X. et al. Regulation of HIV-1 Gag-Pol Expression by Shiftless, an Inhibitor of Programmed -1 Ribosomal Frameshifting. *Cell* 176, 625-635 e614 (2019).

18. Laguette, N. et al. SAMHD1 is the dendritic- and myeloid-cell-specific HIV-1 restriction factor counteracted by Vpx. *Nature* 474, 654-657 (2011).

19. Hrecka, K. et al. Vpx relieves inhibition of HIV-1 infection of macrophages mediated by the SAMHD1 protein. *Nature* 474, 658-661 (2011).

20. Goldstone, D.C. et al. HIV-1 restriction factor SAMHD1 is a deoxynucleoside triphosphate triphosphohydrolase. *Nature* 480, 379-382 (2011).

21. Yu, J. et al. IFITM Proteins Restrict HIV-1 Infection by Antagonizing the Envelope Glycoprotein. *Cell Rep* 13, 145-156 (2015).

22. Liu, S.Y. et al. Interferon-inducible cholesterol-25-hydroxylase broadly inhibits viral entry by production of 25-hydroxycholesterol. *Immunity* 38, 92-105 (2013).

23. Compton, A. et al. IFITM proteins incorporated into HIV-1 virions impair viral fusion and spread. *Cell Host Microbe* 16, 736-747 (2014).

24. Blackshear, P.J. Tristetraprolin and other CCCH tandem zinc-finger proteins in the regulation of mRNA turnover. *Biochem Soc Trans* 30, 945-952 (2002).

25. Sanduja, S., Blanco, F.F. & Dixon, D.A. The roles of TTP and BRF proteins in regulated mRNA decay. *Wiley Interdiscip Rev RNA* 2, 42-57 (2011).

26. Ciais, D., Cherradi, N. & Feige, J.J. Multiple functions of tristetraprolin/TIS11 RNA-binding proteins in the regulation of mRNA biogenesis and degradation. *Cell Mol Life Sci* 70, 2031-2044 (2013).

27. Lai, W.S., Carballo, E., Thorn, J.M., Kennington, E.A. & Blackshear, P.J. Interactions of CCCH zinc finger proteins with mRNA. Binding of tristetraprolin-related zinc finger proteins to Au-rich elements and destabilization of mRNA. *J Biol Chem* 275, 17827-17837 (2000).

28. Stoecklin, G. et al. Functional cloning of BRF1, a regulator of ARE-dependent mRNA turnover. *Embo J* 21, 4709-4718 (2002).

29. Molle, C. et al. Tristetraprolin regulation of interleukin 23 mRNA stability prevents a spontaneous inflammatory disease. *J Exp Med* 210, 1675-1684 (2013).

30. Carballo, E., Lai, W.S. & Blackshear, P.J. Feedback inhibition of macrophage tumor necrosis factor-alpha production by tristetraprolin. *Science* 281, 1001-1005 (1998).

31. Rounbehler, R.J. et al. Tristetraprolin impairs myc-induced lymphoma and abolishes the malignant state. *Cell* 150, 563-574 (2012).

32. Hodson, D.J. et al. Deletion of the RNA-binding proteins ZFP36L1 and ZFP36L2 leads to perturbed thymic development and T lymphoblastic leukemia. *Nat Immunol* 11, 717-724 (2010).

33. Galloway, A. et al. RNA-binding proteins ZFP36L1 and ZFP36L2 promote cell quiescence. *Science* 352, 453-459 (2016).

34. Maeda, M. et al. Tristetraprolin inhibits HIV-1 production by binding to genomic RNA. *Microbes Infect* 8, 2647-2656 (2006).

35. Lin, R.J. et al. Zinc finger protein ZFP36L1 inhibits influenza A virus through translational repression by targeting HA, M and NS RNA transcripts. *Nucleic Acids Res* 48, 7371-7384 (2020).

36. Sutter, K., Dickow, J. & Dittmer, U. Interferon alpha subtypes in HIV infection. *Cytokine Growth Factor Rev* 40, 13-18 (2018).

37. Hardy, G.A. et al. Interferon-alpha is the primary plasma type-I IFN in HIV-1 infection and correlates with immune activation and disease markers. *PLoS One* 8, e56527 (2013).

38. Cha, L. et al. Interferon-alpha, immune activation and immune dysfunction in treated HIV infection. *Clin Transl Immunology* 3, e10 (2014).

39. Brenchley, J.M. et al. Microbial translocation is a cause of systemic immune activation in chronic HIV infection. *Nat Med* 12, 1365-1371 (2006).

40. Wang, S. et al. Neuropilin-1, a myeloid cell-specific protein, is an inhibitor of HIV-1 infectivity. *Proc Natl Acad Sci U S A* 119 (2022).

41. Zhao, L. et al. Vpr counteracts the restriction of LAPTM5 to promote HIV-1 infection in macrophages. *Nat Commun* 12, 3691 (2021).

42. Wang, Q., Zhang, X., Han, Y., Wang, X. & Gao, G. M2BP inhibits HIV-1 virion production in a vimentin filaments-dependent manner. *Sci Rep.* 8 (2016).

43. Liang, G. et al. Membrane metalloprotease TRABD2A restricts HIV-1 progeny production in resting CD4(+) T cells by degrading viral Gag polyprotein. *Nat Immunol* 20, 711-723 (2019).

44. Zhu, Y. et al. Zinc-finger antiviral protein inhibits HIV-1 infection by selectively targeting multiply spliced viral mRNAs for degradation. *Proc Natl Acad Sci U S A.* 108, 15834-15839 (2011).

45. Ellis, M.J. et al. A macrophage-based screen identifies antibacterial compounds selective for intracellular Salmonella Typhimurium. *Nat Commun* 10, 197 (2019).

46. Liang, G. et al. CTNNBL1 restricts HIV-1 replication by suppressing viral DNA integration into the cell genome. *Cell Rep* 38, 110533 (2022).

Acknowledgements

We thank all our laboratory members for their contributions to this study. We would also like to thank Shengjia Li and Yuan Liu for their technical support. This study was supported by the National Science Fund for Distinguished Young Scholars (grant no. 82325034), the National Science Fund for Young Scholars (grant no. 82202599; 82202506), Key Program of the National Natural Science Foundation of China (grant No. 82130069), the Non-profit Central Research Institute Fund of Chinese Academy of Medical Sciences (2023-PT320-01), and the Department of Science and Technology of Liaoning Province Project for the High-Quality Scientific and Technological Development of China Medical University (2023JH2-2020001).

Author contributions

G.L. directed and conceived the research. H.P., H.C., X.Y., and Z.Y. performed the experiments and analyzed the data. H.S. provided intellectual advice on experimental design. G.L. wrote the manuscript.

Competing Interests Statement

The authors declare no competing interests.

FIGURE LEGENDS

Figure 1. ZFP36L2 inhibits HIV-1 production

a,b, 293T cells were co-transfected with pNL4-3 and increasing amounts of FLAG–ZFP36L2 or empty vector. (a) p24 ELISA was performed on supernatants at 48 h.

(b) Cells lysis for immunoblot of ZFP36L2, Gag, gp120, Nef and GAPDH. **c,** 293T cells were co-transfected with the indicated proviral HIV-1 constructs (CXCR4-tropic, CCR5-tropic, or dual-tropic) together with ZFP36L2 or vector control. p24 ELISA was performed on supernatants at 48 h. **d,** Stimulated primary $CD4^+$ T cells were electroporated with a construct encoding FLAG-tagged ZFP36L2 or a mock expression construct, together with HIV-1_{NL4-3}. p24 ELISA was performed at 48 h. **e–g,** Primary $CD4^+$ T cells transduced with GFP-ZFP36L2 or GFP were infected with HIV-1 (10 or 100 ng p24-equivalent). (e) Cell proliferation was assessed by CellTrace Violet at day 8. (f) Viral spread was measured using p24 ELISA. (g) Cells lysis for immunoblot of ZFP36L2 and GAPDH. **h–j,** Primary MDMs transduced with lentiviral ZFP36L2 or mock expression vector were infected with HIV-1_{AD8} (5 or 50 ng p24 equivalent). (h) p24 ELISA was performed over 15 days. (i) Cells lysis for immunoblot of ZFP36L2 and GAPDH. (j) Cytotoxicity was measured by LDH release. **k–p,** 293T cells were transfected with a construct encoding FLAG-tagged ZFP36L2 or a mock expression construct, together with the indicated proviral vectors (HIV-2, SIV, EIAV, FIV, MLV, or HBV). (k) HIV-2 RT activity. (l) SIV p27 ELISA. (m) EIAV RT activity. (n) FIV late RT products measured by qPCR. (o) MLV late RT products measured by qPCR. (p) HBV virion DNA measured by qPCR. All data are mean ± s.d and represent three independent experiments. unpaired two-tailed Student's t-test was used for (j) and the two-way ANOVA with Šidák's multiple comparison tests was used for the other. No adjustments were made for multiple comparisons beyond the post hoc tests specified. Two-tailed, all $p < 0.0001$ or =0.0001, ns: not significant. All western blotting data are representative of three independent experiments. Source data are provided as a Source Data file.

Figure 2. ZFP36L2 inhibits nuclear export of RRE-containing HIV-1 RNA.

a–c, 293T cells were co-transfected with HIV-$1_{NL4\text{-}3.Luc.R-E-}$ and increasing amounts of FLAG-ZFP36L2 or vector control. (a) Luciferase activity was measured at 24 h. (b) Total, nuclear and cytoplasmic gag RNA were quantified by RT-qPCR ($p < 0.0001$; n = 3). (c) Cells lysis for immunoblot of ZFP36L2, Gag, Lamin B and GAPDH; RT-PCR was performed to detect *U6* snRNA and *GAPDH*. **d–g,** 293T cells were co-transfected with HIV-$1_{NL4\text{-}3}$ proviral vectors and ZFP36L2 or vector control. (d) Schematic of HIV-1 transcripts, with the *RRE* indicated in red. (e) Nuclear and cytoplasmic viral RNAs were measured by RT-qPCR ($p < 0.0001$; n = 3). (f) Primer strategy showing forward primer (FP) and reverse primers (RP1 and RP2), as indicated. (g) RT-PCR followed by Southern blotting of total, nuclear and cytoplasmic RNA. **h,i,** Cells lysis for immunoblot (h) and RT-PCR (i) validation of fractionation. All data are mean ± s.d and represent three independent experiments. Two-way ANOVA with Šidák's multiple comparisons test was used for (a, b, e). All test were two-tailed, ** $p < 0.01$, ns: not significant, BD, below the detection limit. All western and southern blotting data are representative of three independent experiments. Source data are provided as a Source Data file.

Figure 3. ZFP36L2 restricts HIV-1 expression in a Rev-dependent manner.

a, Schematic of *Gag-Pol* and *Gag-Pol-RRE* transcripts derived from their expression vectors. **b–e,** 293T cells were co-transfected with ZFP36L2 or vector control, together with *Gag-Pol* (b,c) or *Gag-Pol-RRE* (d,e) expression vector. At 24 h post-transfection, nuclear and cytoplasmic RNA were isolated for RT–qPCR analysis to quantify HIV-1

transcript copies, normalized to GAPDH in the presence or absence of reverse transcriptase. Total RNA levels were calculated as the sum of nuclear and cytoplasmic RNA (b,d). Cells lysis for immunoblot of ZFP36L2, Gag, Lamin B and GAPDH (c,e). **f,** 293T cells were cotransfected with a FLAG-tagged Rev expression construct, together with GFP-tagged ZFP36L2 or mock (GFP) expression vectors. At 24 h post-cotransfection, cells were lysed and treated with or without benzonase prior to IP assays using anti-FLAG (left) or anti-GFP (right) antibodies. Western blotting was performed to detect FLAG-Rev, GFP, and ZFP36L2-GFP. **g–i,** HeLa cells were cotransfected with GFP-tagged ZFP36L2 or mock expression vectors along with Rev-defective NL4-3-Δ*rev* proviral vectors in the presence or absence of FLAG-tagged wild-type or mutant Rev (Δ109-116) expression constructs. (g) p24 ELISA was performed at 24 h ($p < 0.0001$; n = 3). (h) Nuclear and cytoplasmic *gag* RNA levels were quantified by RT-qPCR ($p < 0.0001$; n = 3). (i) Cells lysis for immunoblot of ZFP36L2, Rev, Gag, Lamin B and GAPDH. All data are presented as mean ± s.d. from three independent experiments. Two-way ANOVA with Šidák's multiple comparisons test was used for (b, d, g, h). All tests were two-tailed, ** $p < 0.01$ ns: not significant, BD, below the detection limit. All western blotting data are representative of three independent experiments. Source data are provided as a Source Data file.

Figure 4. ZFP36L2 does not affect HIV-1*Rev(Δ109-116)* replication.

a, HeLa cells were cotransfected with FLAG-tagged ZFP36L2 and mock constructs along with wild-type or *rev(Δ109-116)* mutant HIV-1 proviral vectors. At 24 h post-cotransfection, the HIV-1 capsid protein in culture were measured using p24 ELISA. **b–e,** Jurkat T cells

(b,c) or stimulated $CD4^+$ T (d,e) were electroporated with FLAG-tagged ZFP36L2 and mock constructs along with wild-type or *rev(Δ109-116)* mutant HIV-1 proviral vectors in the presence of 300 nM raltegravir. At 48 h post-electroporation, the levels of HIV-1 capsid protein in culture were measured using p24 ELISA (b,d). Cells were lysed for western blotting to assess ZFP36L2 and GAPDH expression (c,e). **f,g,** Lentiviral GFP-tagged ZFP36L2 or GFP expression vector-transduced Jurkat cells were infected with 10 ng (low dose) or 100 ng (high dose) of p24-equivalent wild-type or Rev (Δ109-116) mutant HIV-1_{NL4-3} for 8 days. Viral production in culture was measured using p24 ELISA at the indicated time points (f). Cells were lysed for western blotting to assess ZFP36L2, GFP, and GAPDH expression (g). **h,i,** Lentiviral GFP-tagged ZFP36L2 or Mock (GFP) expression vector-transduced stimulated $CD4^+$ T cells (CD3CD28 + IL2) were infected with 20 ng of p24-equivalent wild-type or Rev (Δ109-116) mutant HIV-1_{NL4-3} for 8 days. Viral production in culture was measured using p24 ELISA at the indicated time points (h). Cells were lysed for western blotting to assess ZFP36L2 and GAPDH expression (i). *P* values were calculated using the two-way ANOVA with Šidák's multiple comparison tests. ** $p < 0.01$, ns: not significant. The data points are means with SD and represent three independent experiments. All western blotting data are representative of three independent experiments. Source data are provided as a Source Data file.

Figure 5. IFN-β, but not IFN-α, induces ZFP36L2 to restrict HIV-1 infection.

a,b, The inhibitory effect of IFN-β is impaired in the absence of ZFP36L2. Lentiviral shRNA-transduced stimulated $CD4^+$ T cells were treated with or without IFN-α or IFN-β (1000 U/ml). At 48 h post-treatment, cells were infected with 10 or 25 ng of p24-equivalent

HIV-$1_{NL4-3.Luc}$ (VSV-G) in the presence or absence of EFV (300 nM). At 6 h post-infection, cells were washed and replenished with culture media containing either IFN-α or IFN-β (1000 U/ml) or without IFN. At 48 h post-infection, viral production was measured using p24 ELISA (a). The aliquoted cells were lysed for western blotting to assess ZFP36L2, Gag, and GAPDH levels (b). **c,d,** The inhibitory effect of IFN-β on HIV-$1_{Rev(Δ109-116)}$ replication is impaired. Stimulated $CD4^+$ T cells were treated with or without IFN-α or IFN-β at 1000 U/ml. At 48 h post-treatment, cells were infected with 10 ng (c) or 100 ng (d) of p24-equivalent wild-type or Rev mutant HIV-1_{NL4-3}. At 6 h post-infection, cells were washed and replenished with culture media either IFN-α or IFN-β at 1000 U/ml or without IFN. At 72 h post-infection, viral production was measured using p24 ELISA. **e,f,** HIV-$1_{Rev(Δ109-116)}$ replication was not affected by the IFN-β-induced ZFP36L2. Lentiviral shRNA-transduced stimulated $CD4^+$ T cells were treated with or without IFN-α or IFN-β (1000 U/ml). At 48 h post-treatment, cells were infected with 100 ng of p24-equivalent wild-type or *Rev (Δ109-116)* mutant HIV-1_{NL4-3}. At 6 h post-infection, cells were washed and replenished with culture media containing either IFN-α or IFN-β (1000 U/ml) or without IFN. At 48 h post-infection, viral production was measured using p24 ELISA (e). The aliquoted cells were lysed for western blotting to assess ZFP36L2, Gag, and GAPDH levels (f). *P* values were calculated using the two-way ANOVA with Šidák's multiple comparison tests. ** $p < 0.01$, BD, below the detection limit. The data points are means with SD and represent three independent experiments. All western blotting data are representative of three independent experiments. Source data are provided as a Source Data file.

Figure 6. IFN-β induces ZFP36L2 to restrict HIV-1 spread in CD4⁺ T cells from patients.

a, ZFP36L2 mRNA levels in CD4⁺ T cells from healthy donors (n = 15), cART-treated individuals (n = 24; VL < 50 copies/mL), and untreated people living with HIV (n = 30), measured by qRT–PCR ($p = 0.0005$, healthy vs. untreated; $p < 0.0001$, cART-treated vs. untreated). **b–d,** Correlations in untreated individuals (n = 30) between ZFP36L2 mRNA and plasma viral load (b; $p = 0.0019$), CD4 count (c; $p = 0.0097$), or CD4/CD8 ratio (d; $p = 0.51$), analyzed by two-tailed Spearman's rank test. **e,** Experimental schematic for panel f–h. **f–h,** CD4⁺ T cells from two ART-naive or ART-treated individuals were transduced with wild-type or Δ446–480 ZFP36L2–GFP, or GFP vector control. (f) Proliferation was assessed by CellTrace Violet (day 8). (g) Viral production was measured using TZM-bl reporter cells (n = 3 technical replicates). (h) Immunoblot of ZFP36L2 and GAPDH. **i–k,** CD4⁺ T cells from ART-naive individuals (n = 17) were transduced with shZFP36L2 or shCtrl and cultured ± IFN-β (1000 U/mL). (i) HIV-1 titers were measured using TZM-bl cells ($p = 0.0495$). (j) ZFP36L2 mRNA was quantified by qPCR ($p = 0.0003$). (k) Proliferation was assessed by CellTrace Violet. **l–n,** The same procedure was performed using CD4⁺ T cells from ART-treated individuals (n = 23). (l) HIV-1 titers ($p < 0.0001$). (m) ZFP36L2 mRNA levels ($p < 0.0001$). (n) Proliferation by CellTrace Violet. Data are mean ± s.d. (a,g) or s.e.m. (i,j,l,m) and represent three or more independent experiments. Statistical analyses included one-way ANOVA with Dunnett's test (a), Spearman correlation (b–d) and two-way ANOVA with Šidák's multiple comparisons test (g, i, j, l, m). No adjustments were made for multiple comparisons beyond the specified post hoc tests.

Two-tailed, * $p < 0.05$, ** $p < 0.01$, *** $p < 0.001$, ns: not significant. Source data are provided as a Source Data file.

Type I interferons play important in the innate immune response to HIV-1 infection. Here the authors suggest that nuclear RNA binding protein ZFP36L2 is induced by interferon-β and acts to restrict the nuclear export of HIV-1 transcripts.

Peer review information: *Nature Communications* thanks Stuart Neil, and the other, anonymous, reviewer(s) for their contribution to the peer review of this work. A peer review file is available.

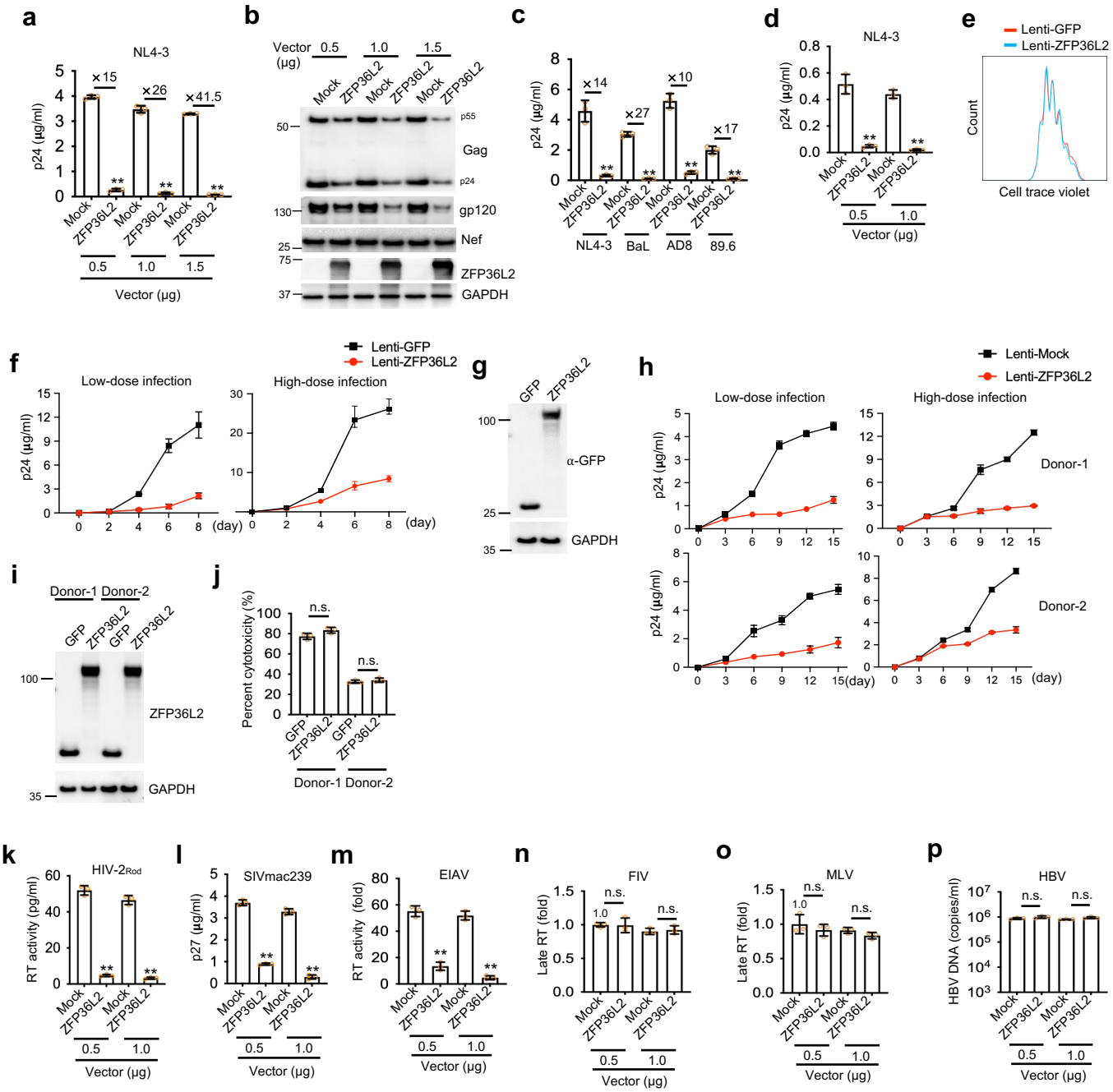
a
NL4-3
p24 (μg/ml)
×15
×26
×41.5
Mock
ZFP36L2
0.5
1.0
1.5
Vector (μg)
b
Vector (μg)
0.5
1.0
1.5
p55
Gag
p24
gp120
Nef
ZFP36L2
GAPDH
c
×14
×27
×10
×17
NL4-3
BaL
AD8
89.6
d
NL4-3
e
Lenti-GFP
Lenti-ZFP36L2
Count
Cell trace violet
f
Low-dose infection
High-dose infection
(day)
g
GFP
ZFP36L2
α-GFP
h
Lenti-Mock
Donor-1
Donor-2
i
Donor-1
Donor-2
j
Percent cytotoxicity (%)
n.s.
k
HIV-2Rod
RT activity (pg/ml)
l
SIVmac239
p27 (μg/ml)
m
EIAV
RT activity (fold)
n
FIV
Late RT (fold)
o
MLV
p
HBV
HBV DNA (copies/ml)

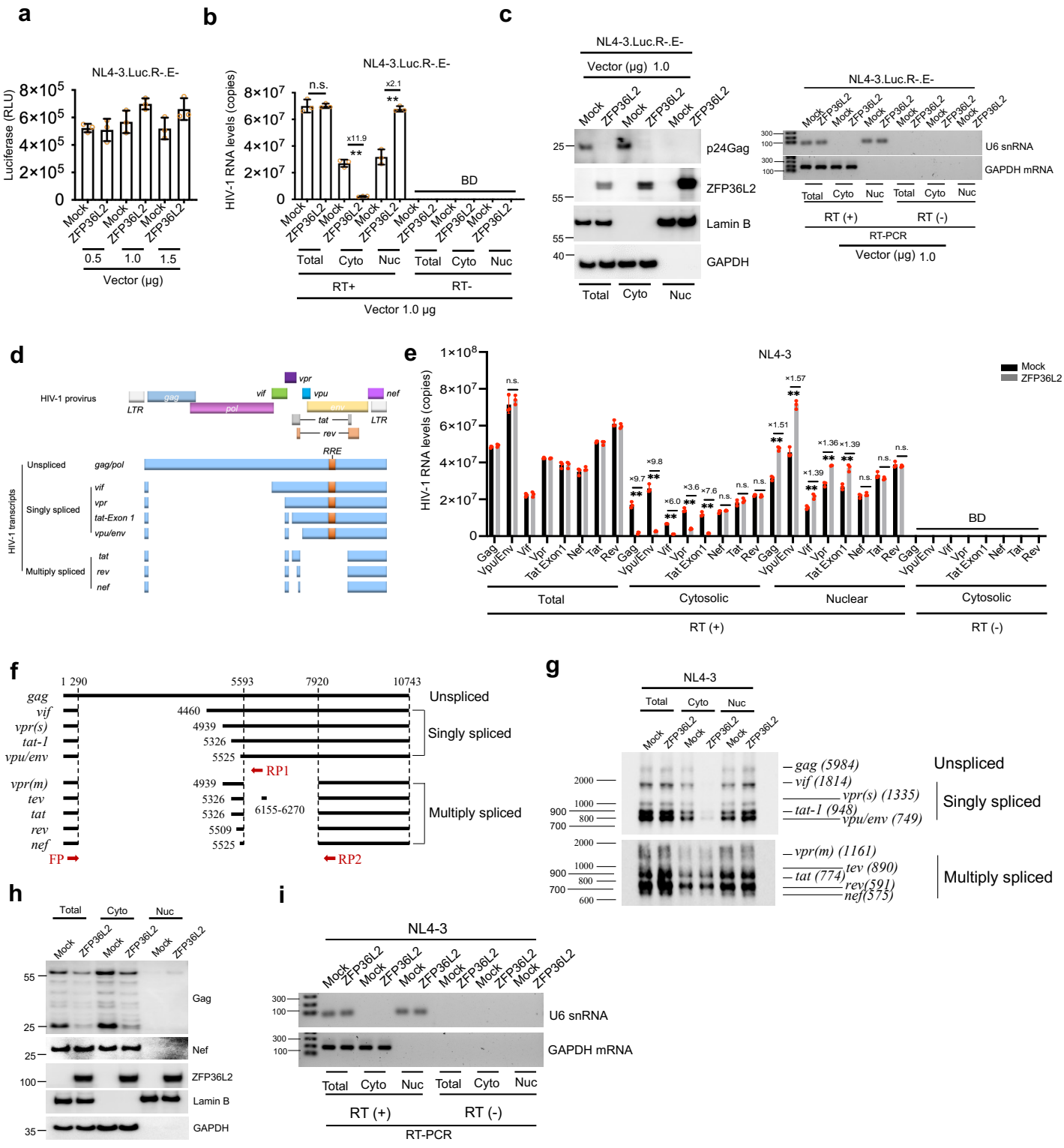
a
NL4-3.Luc.R-.E-
Luciferase (RLU)
Vector (μg)
b
NL4-3.Luc.R-.E-
HIV-1 RNA levels (copies)
n.s.
x11.9
x2.1
BD
Total
Cyto
Nuc
RT+
RT-
Vector 1.0 μg
c
NL4-3.Luc.R-.E-
Vector (μg) 1.0
p24Gag
ZFP36L2
Lamin B
GAPDH
U6 snRNA
GAPDH mRNA
RT (+)
RT (-)
RT-PCR
d
HIV-1 provirus
LTR
gag
pol
vif
vpu
env
vpr
tat
rev
nef
RRE
HIV-1 transcripts
Unspliced
gag/pol
Singly spliced
vif
vpr
tat-Exon 1
vpu/env
Multiply spliced
tat
rev
nef
e
NL4-3
HIV-1 RNA levels (copies)
Mock
ZFP36L2
Gag
Vpu/Env
Vif
Vpr
Tat Exon1
Nef
Tat
Rev
Total
Cytosolic
Nuclear
RT (+)
RT (-)
f
1 290
5593
7920
10743
gag
vif
vpr(s)
tat-1
vpu/env
vpr(m)
tev
tat
rev
nef
4460
4939
5326
5525
RP1
6155-6270
5509
RP2
FP
Unspliced
Singly spliced
Multiply spliced
g
NL4-3
Total
Cyto
Nuc
gag (5984)
vif (1814)
vpr(s) (1335)
tat-1 (948)
vpu/env (749)
vpr(m) (1161)
tev (890)
tat (774)
rev(591)
nef(575)
Unspliced
Singly spliced
Multiply spliced
h
Total
Cyto
Nuc
Gag
Nef
ZFP36L2
Lamin B
GAPDH
i
NL4-3
U6 snRNA
GAPDH mRNA
RT (+)
RT (-)
RT-PCR

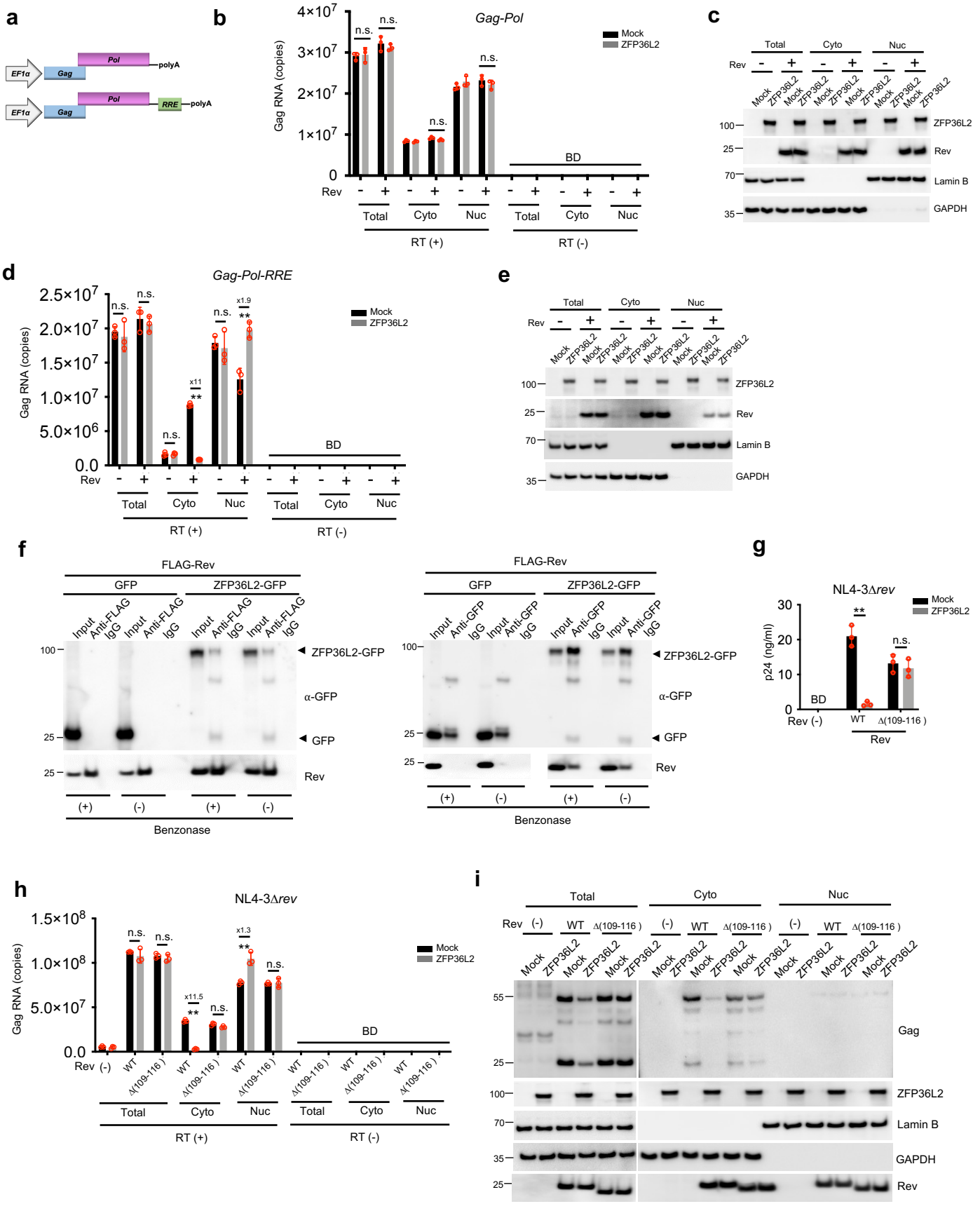
a
EF1α
Gag
Pol
polyA
RRE
b
Gag-Pol
Gag RNA (copies)
Mock
ZFP36L2
n.s.
BD
Rev
Total
Cyto
Nuc
RT (+)
RT (-)
c
Total
Cyto
Nuc
Rev
Mock
ZFP36L2
100
25
70
35
Lamin B
GAPDH
d
Gag-Pol-RRE
x11
x1.9
e
f
FLAG-Rev
GFP
ZFP36L2-GFP
Input
Anti-FLAG
IgG
Anti-GFP
α-GFP
GFP
Rev
Benzonase
(+)
(-)
g
NL4-3Δrev
p24 (ng/ml)
BD
WT
Δ(109-116)
h
NL4-3Δrev
x11.5
x1.3
i
Gag

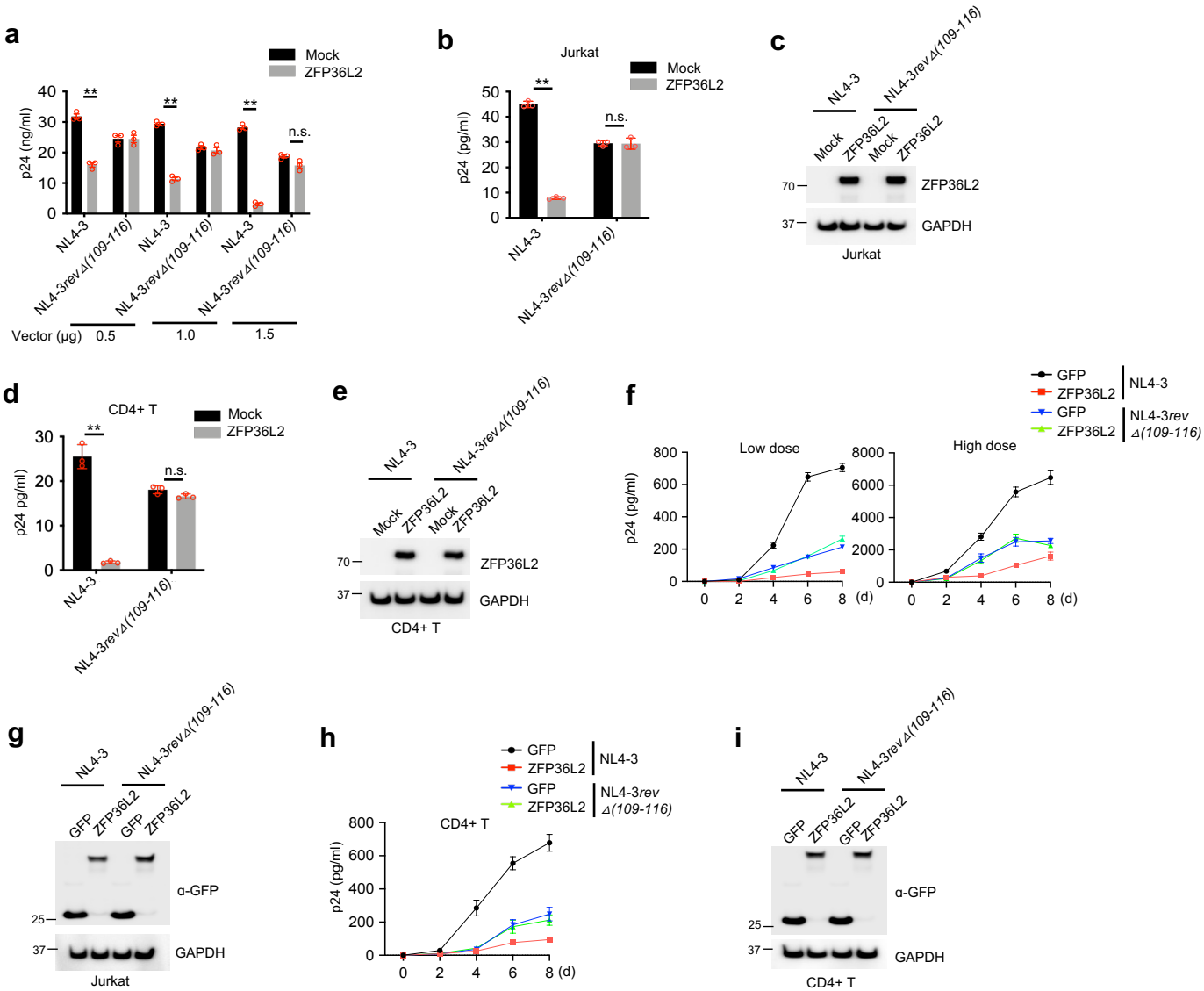
a
Mock
ZFP36L2
p24 (ng/ml)
**
n.s.
NL4-3
NL4-3revΔ(109-116)
Vector (μg) 0.5 1.0 1.5
b
Jurkat
p24 (pg/ml)
c
NL4-3
NL4-3revΔ(109-116)
Mock
ZFP36L2
70
37
ZFP36L2
GAPDH
Jurkat
d
CD4+ T
e
CD4+ T
f
GFP
ZFP36L2
NL4-3
NL4-3rev Δ(109-116)
Low dose
High dose
p24 (pg/ml)
(d)
g
α-GFP
GAPDH
Jurkat
h
CD4+ T
i
CD4+ T

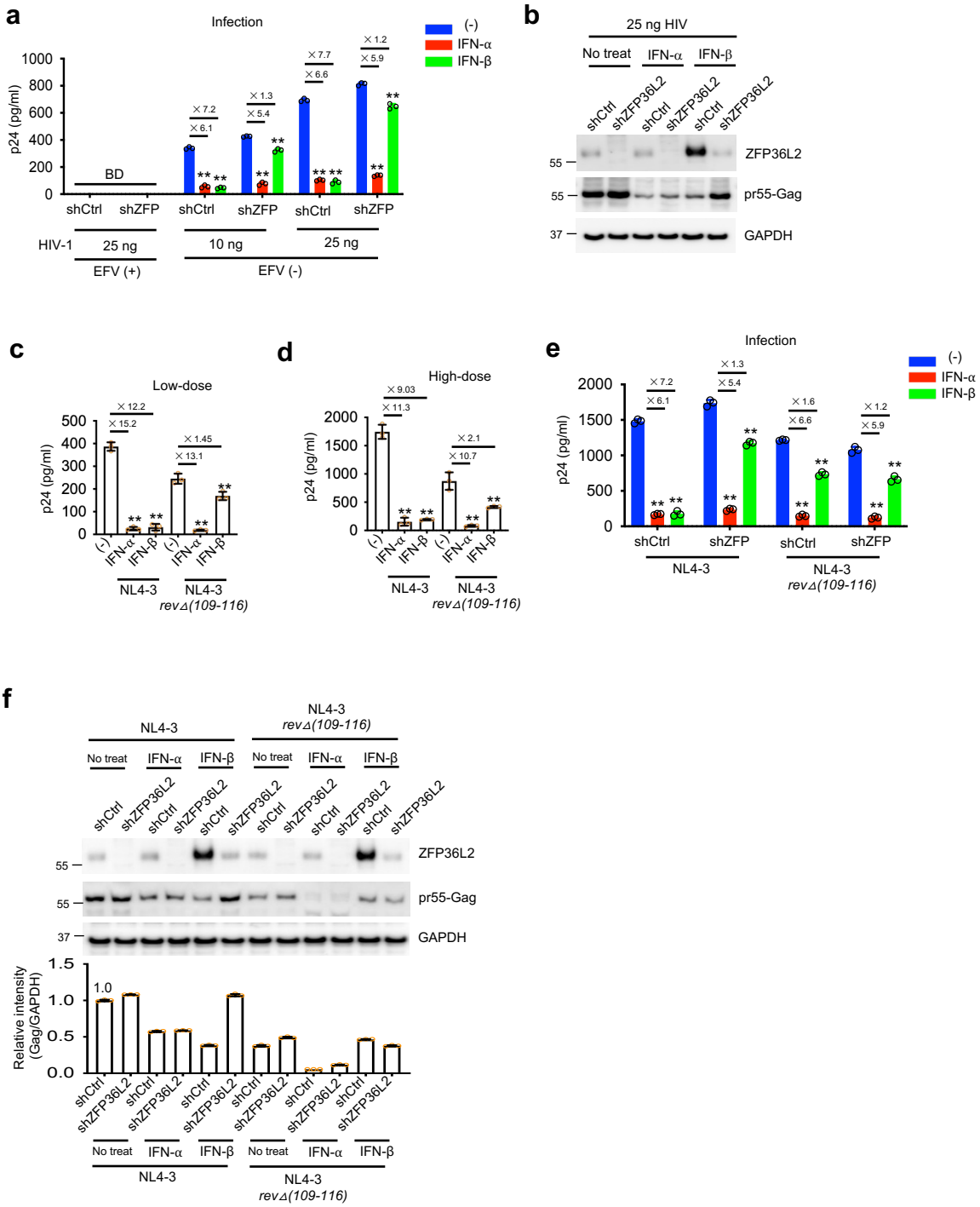
a
Infection
(-)
IFN-α
IFN-β
p24 (pg/ml)
1000
800
600
400
200
0
BD
×7.2
×6.1
×1.3
×5.4
×7.7
×6.6
×1.2
×5.9
shCtrl
shZFP
HIV-1
25 ng
10 ng
25 ng
EFV (+)
EFV (-)
b
25 ng HIV
No treat
IFN-α
IFN-β
shCtrl
shZFP36L2
55
ZFP36L2
pr55-Gag
37
GAPDH
c
Low-dose
×12.2
×15.2
×1.45
×13.1
NL4-3
NL4-3
revΔ(109-116)
d
High-dose
×9.03
×11.3
×2.1
×10.7
e
Infection
×7.2
×6.1
×1.3
×5.4
×1.6
×6.6
×1.2
×5.9
f
NL4-3
NL4-3
revΔ(109-116)
Relative intensity
(Gag/GAPDH)
1.5
1.0
0.5
0.0
1.0

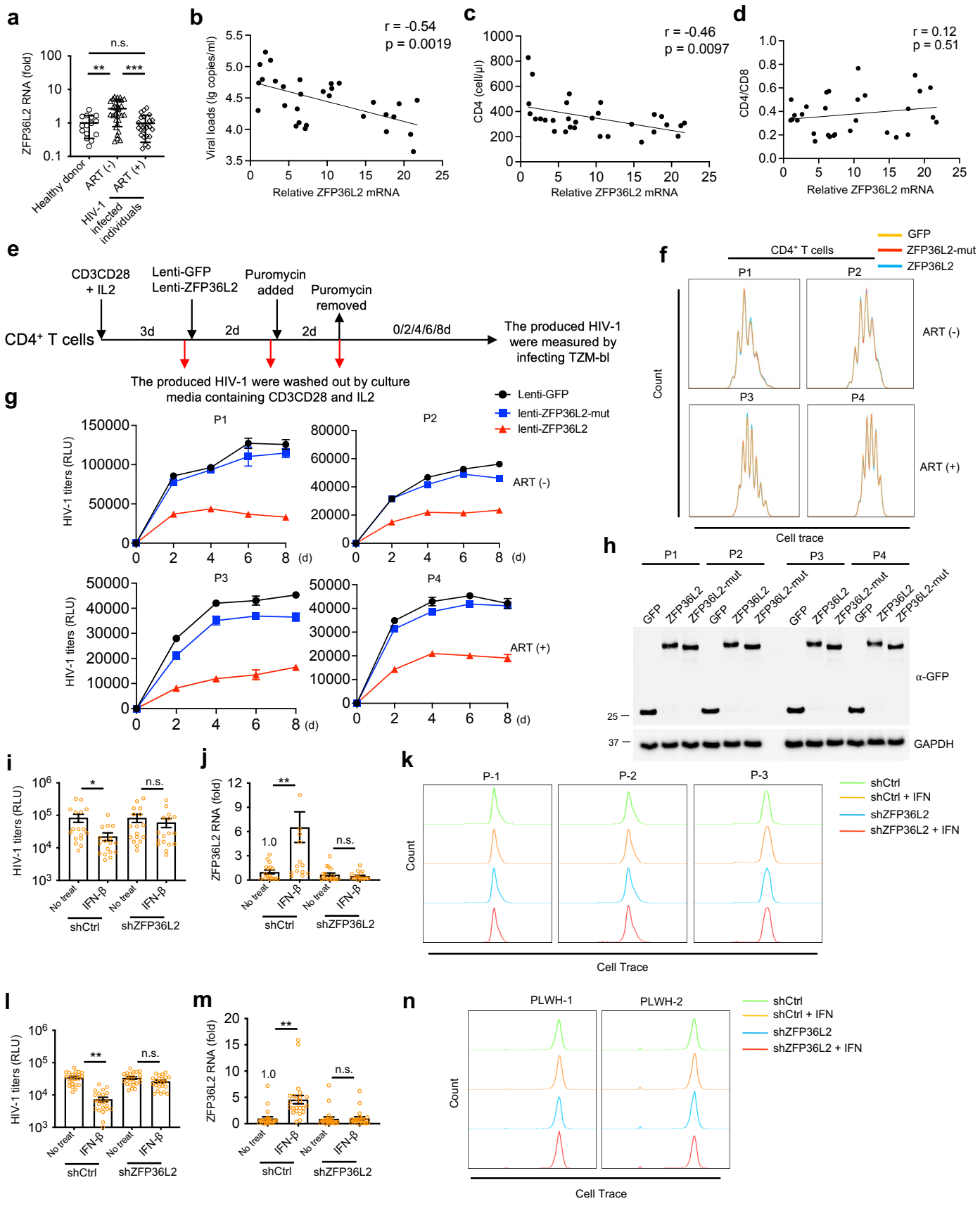
a
ZFP36L2 RNA (fold)
n.s.
**
***
Healthy donor
ART (-)
ART (+)
HIV-1 infected individuals
b
Viral loads (lg copies/ml)
r = -0.54
p = 0.0019
Relative ZFP36L2 mRNA
c
CD4 (cell/μl)
r = -0.46
p = 0.0097
Relative ZFP36L2 mRNA
d
CD4/CD8
r = 0.12
p = 0.51
Relative ZFP36L2 mRNA
e
CD3CD28 + IL2
Lenti-GFP
Lenti-ZFP36L2
Puromycin added
Puromycin removed
CD4+ T cells
3d
2d
2d
0/2/4/6/8d
The produced HIV-1 were measured by infecting TZM-bl
The produced HIV-1 were washed out by culture media containing CD3CD28 and IL2
f
CD4+ T cells
GFP
ZFP36L2-mut
ZFP36L2
P1
P2
P3
P4
ART (-)
ART (+)
Count
Cell trace
g
Lenti-GFP
lenti-ZFP36L2-mut
lenti-ZFP36L2
HIV-1 titers (RLU)
ART (-)
ART (+)
(d)
h
α-GFP
GAPDH
25
37
i
HIV-1 titers (RLU)
No treat
IFN-β
shCtrl
shZFP36L2
j
ZFP36L2 RNA (fold)
1.0
k
shCtrl
shCtrl + IFN
shZFP36L2
shZFP36L2 + IFN
Count
Cell Trace
l
m
n
PLWH-1
PLWH-2